

A sequence stratigraphic model for an intensely bioturbated shallow-marine sandstone: the Bridport Sand Formation, Wessex Basin, UK

JENNY E. MORRIS, GARY J. HAMPSON and HOWARD D. JOHNSON

Department of Earth Sciences and Engineering, Imperial College London, South Kensington Campus, London SW7 2AZ, UK (E-mail: jenny.morris@imperial.ac.uk)

ABSTRACT

The Bridport Sand Formation is an intensely bioturbated sandstone that represents part of a mixed siliciclastic-carbonate shallow-marine depositional system. At outcrop and in subsurface cores, conventional facies analysis was combined with ichnofabric analysis to identify facies successions bounded by a hierarchy of key stratigraphic surfaces. The geometry of these surfaces and the lateral relationships between the facies successions that they bound have been constrained locally using 3D seismic data. Facies analysis suggests that the Bridport Sand Formation represents progradation of a low-energy, siliciclastic shoreface dominated by storm-event beds reworked by bioturbation. The shoreface sandstones form the upper part of a thick (up to 200 m), steep (2–3°), mud-dominated slope that extends into the underlying Down Cliff Clay. Clinoform surfaces representing the shoreface-slope system are grouped into progradational sets. Each set contains clinoform surfaces arranged in a downstepping, offlapping manner that indicates forced-regressive progradation, which was punctuated by flooding surfaces that are expressed in core and well-log data. In proximal locations, progradational shoreface sandstones (corresponding to a clinoform set) are truncated by conglomerate lags containing clasts of bored, reworked shoreface sandstones, which are interpreted as marking sequence boundaries. In medial locations, progradational clinoform sets are overlain across an erosion surface by thin (<5 m) bioclastic limestones that record siliciclastic-sediment starvation during transgression. Near the basin margins, these limestones are locally thick (>10 m) and overlie conglomerate lags at sequence boundaries. Sequence boundaries are thus interpreted as being amalgamated with overlying transgressive surfaces, to form composite erosion surfaces. In distal locations, oolitic ironstones that formed under conditions of extended physical reworking overlie composite sequence boundaries and transgressive surfaces. Over most of the Wessex Basin, clinoform sets (corresponding to high-frequency sequences) are laterally offset, thus defining a low-frequency sequence architecture characterized by high net siliciclastic sediment input and low net accommodation. Aggradational stacking of high-frequency sequences occurs in fault-bounded depocentres which had higher rates of localized tectonic subsidence.

Keywords: Bridport Sand Formation, clinoform, facies architecture, ichnofacies analysis, sequence stratigraphy.

INTRODUCTION

Intensely bioturbated shallow marine sandstones are a common feature of the stratigraphic record, but interpretation of their internal facies architecture and depositional environments is often hampered by a lack of primary sedimentary structures. Consequently, their high-resolution sequence stratigraphic context and significance are poorly understood, resulting in a paucity of predictive depositional models. This paper presents a high-resolution sequence stratigraphic model for one such intensely bioturbated shallow-marine sandstone of enigmatic origin; the Bridport Sand Formation (BSF) of the Wessex Basin, UK. The unit is upward-coarsening and is composed of friable, very fine- to fine-grained siliciclastic sandstones of variable silt content. Primary sedimentary structures have largely been destroyed by pervasive bioturbation, but where preserved, they are interpreted as recording wave and/or storm processes (Davies, 1969; Kantorowicz *et al.*, 1987; Bryant *et al.*, 1988; Pickering, 1995). The BSF also contains thin (<1 m), closely spaced (<2 m vertical spacing), laterally extensive carbonate-cemented horizons rich in bioclastic debris. Previous workers have interpreted the BSF as the deposits of submerged, storm-dominated shelf bars (Bryant *et al.*, 1988), the distal part of a storm-dominated shoreface and inner shelf (Colter & Havard, 1981; Hounslow, 1987), and a migrating barrier shoreline and back-barrier lagoon (Davies, 1969). The regional extent and geometry of the unit are also poorly constrained and poorly understood (Hesselbo & Jenkyns, 1995; Ainsworth *et al.*, 1998b; Buchanan, 1998; Hawkes *et al.*, 1998). The integrated data set presented here, including new 3D seismic data, and an analytical approach combining conventional facies interpretation, ichnofabric analysis and sequence stratigraphy have allowed depositional environments, stratal architecture and palaeogeography to be more closely constrained. The resulting sequence stratigraphic model has direct applications to improved understanding of the architecture of the BSF reservoir in the Wytch Farm Oilfield (Colter & Havard, 1981), and also to predictions of BSF reservoir distribution in the Wessex Basin (e.g. Buchanan, 1998). Moreover, the model is largely generic and aspects of it can be applied to other enigmatic, intensely bioturbated shallow-marine sandstones (e.g. the Middle Jurassic Tarbert, Emerald, Sognefjord and Fensfjord formations and the Upper Jurassic Fulmar and Ula formations, North Sea).

The aims of this paper were twofold: (i) to construct a sequence stratigraphic model that is compatible with both small-scale facies successions and discontinuity surfaces identified in core and outcrop, and also large-scale stratal geometries identified in seismic data, and (ii) to illustrate the application of ichnology to sequence stratigraphy by identifying facies variations in an apparently homogenous, intensely bioturbated, shallow marine sandstone.

DATA SET AND METHODS

This study uses an integrated data set that combines data from the Wytch Farm Field together with regional data collected throughout the Wessex Basin south of the Mendip Axis (Fig. 1). The data set includes over 650 m of core from 12 wells (seven within the Wytch Farm Field and five regional wells), outcrop sections, 160 km of 2D regional seismic lines, 3D seismic data covering an area of 150 km², and wireline log data from 126 wells. Description and interpretation of cores and outcrops was based on conventional facies analysis methods combined with detailed ichnological analysis. Palynological samples were analysed to test environmental interpretations of two mud-prone facies. Key stratigraphic surfaces have been identified in cores and outcrops, and assigned to a hierarchy according to the magnitude of facies dislocation interpreted across them. The wireline-log expression of these surfaces has been characterized, principally using gamma-ray and sonic logs. A 3D seismic data set from the Wytch Farm Field, which was produced in 1998 by merging older offshore and onshore surveys, has been used to study stratal geometries (Fig. 1B). 3D seismic data quality deteriorates in the eastern, offshore part of the area (Fig. 1B). Depth migration studies, which involved the generation of synthetic wavelet responses from sonic and density logs in two wells, have been used to tie surfaces identified in well data (wireline logs, cores) to the 3D seismic volume. The resolution of regional 2D seismic data is too low to enable stratal architecture to be imaged in the BSF outside of the Wytch Farm Field, although the base and top of the stratigraphic interval that contains it [i.e. an interval comprising the Down Cliff Clay (DCC), BSF and the Inferior Oolite Formation (IOF), Fig. 2] can be readily identified. Thus, regional thickness variations were studied using selected 2D seismic

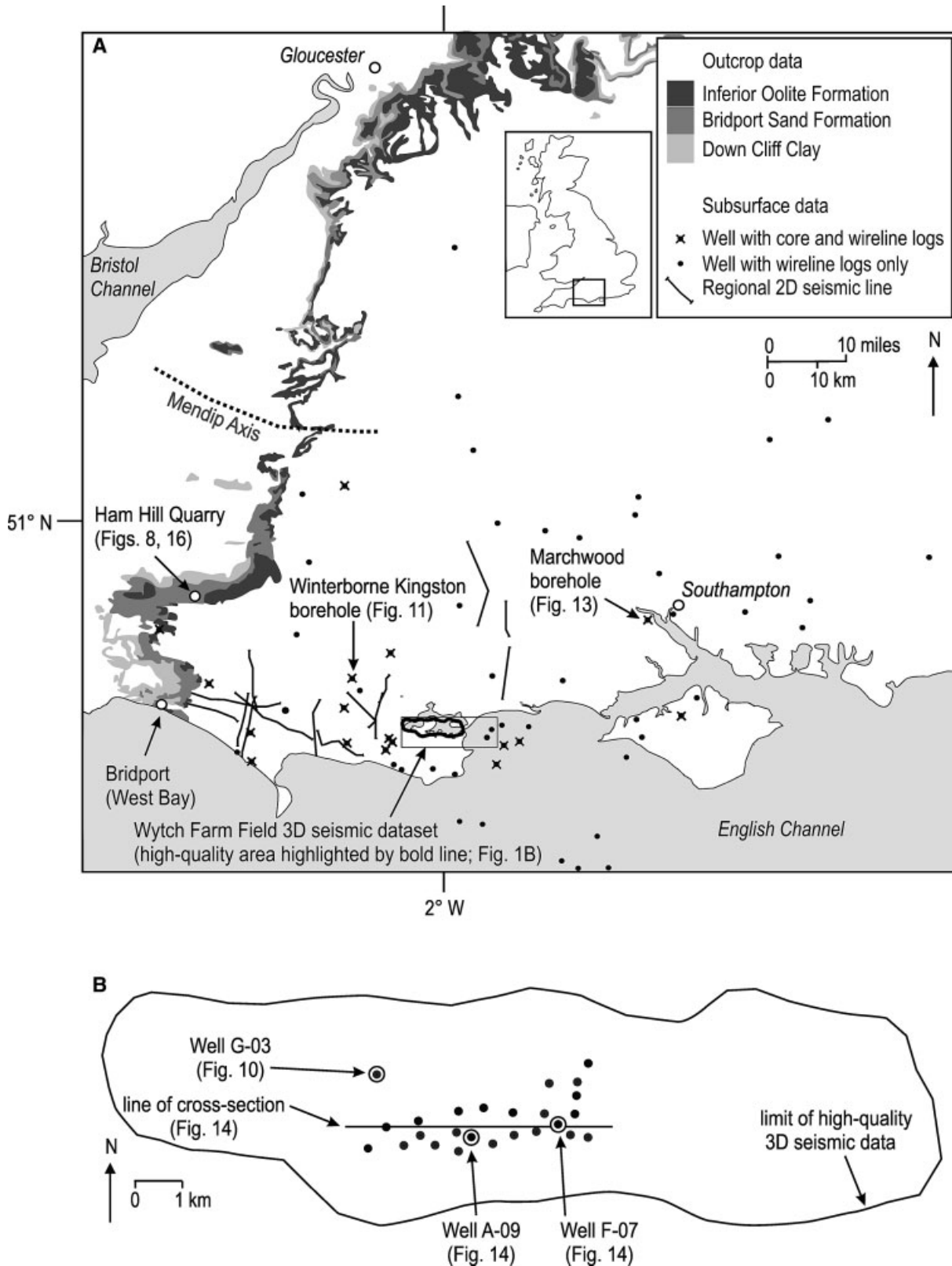


Fig. 1. (A) Map of central southern England illustrating the distribution of the integrated data set used for this study: (1) coastal outcrops in the Bridport area, (2) Ham Hill Quarry and other inland outcrops, (3) detailed subsurface data (e.g. 3D seismic) from the Wytch Farm oil field and (4) regional subsurface data (e.g. wells and 2D seismic). (B) Detailed map of the Wytch Farm field showing the areal extent of 3D seismic and well-log data.

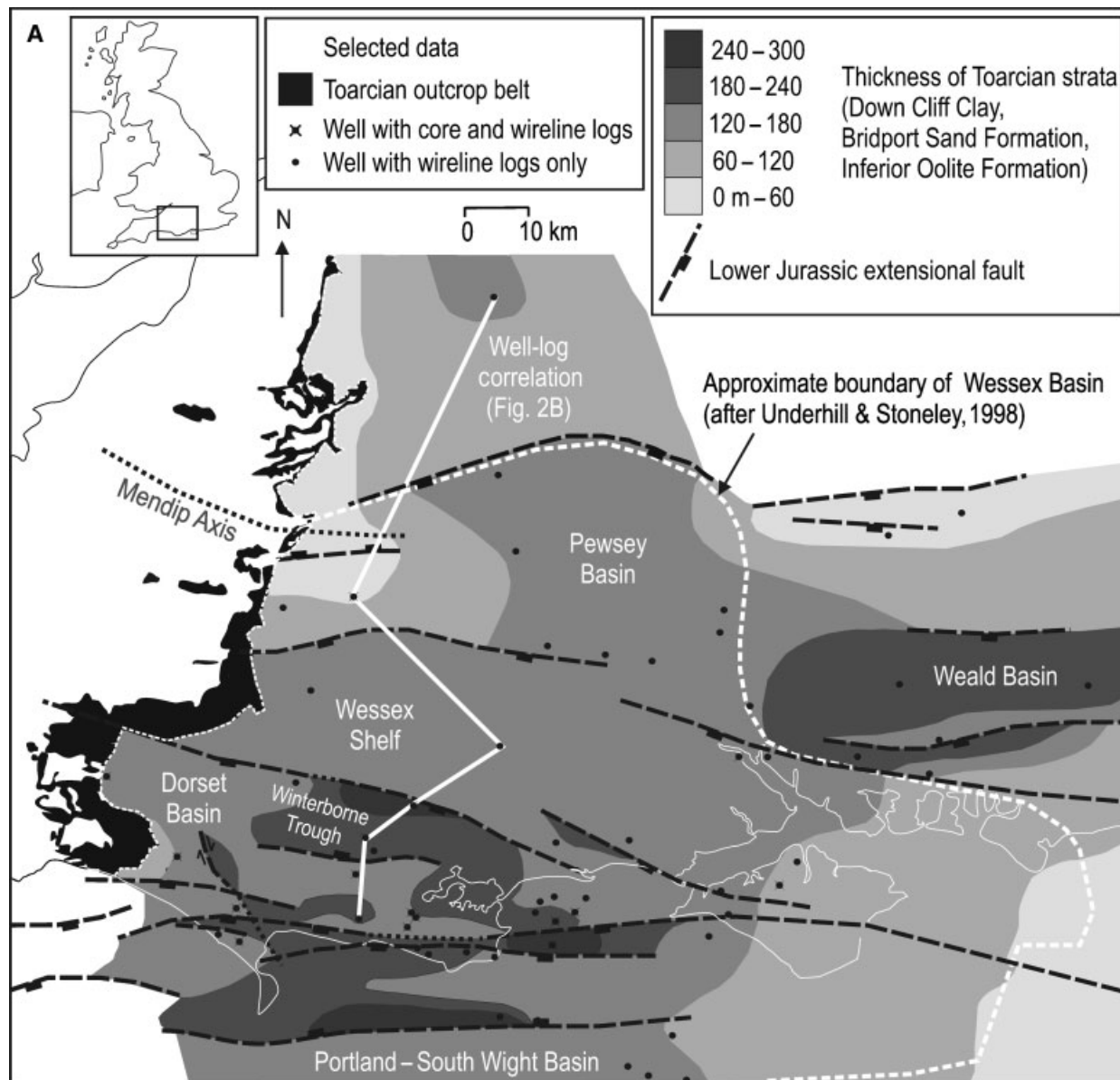


Fig. 2. (A) Isopach map illustrating variations in thickness of the Toarcian strata (Down Cliff Clay, Bridport Sand Formation and Inferior Oolite Formation) across the Wessex Basin. Fault distributions and thickness patterns are based on Hawkes *et al.* (1998), in addition to the study data set. Note that the strata thicken across east–west-trending faults that bound the Pewsey Basin, Wessex Shelf, Winterborne Trough and Portland–South Wight Basin. (B) Regional well-log cross-section illustrating thickness variations of Toarcian strata in relation to the main structural elements. These strata form a large-scale regressive–transgressive cycle (Hesselbo & Jenkyns, 1998). Gamma ray (GR, in API units) and sonic logs (DT, in $\mu\text{s}/\text{ft}$) are shown for each well.

sections and correlations of lithostratigraphic units between widely spaced wells.

Although the data set described above is large and contains a wide variety of data types, it is not without shortcomings. Firstly, outcrop and core data allow very detailed vertical facies trends to be studied, but these data are only available for a few isolated areas. Most cores are clustered within the Wytch Farm Field, and high-quality

exposures are limited to coastal cliffs near Bridport and inland quarries near Yeovil (Fig. 1A). Secondly, 3D seismic data are only available over the Wytch Farm Field and offer much higher resolution than the regional 2D seismic data. The approach adopted here has therefore been driven by data density and quality. Vertical facies trends have been interpreted in all cores and outcrops, and within the Wytch Farm Field such trends

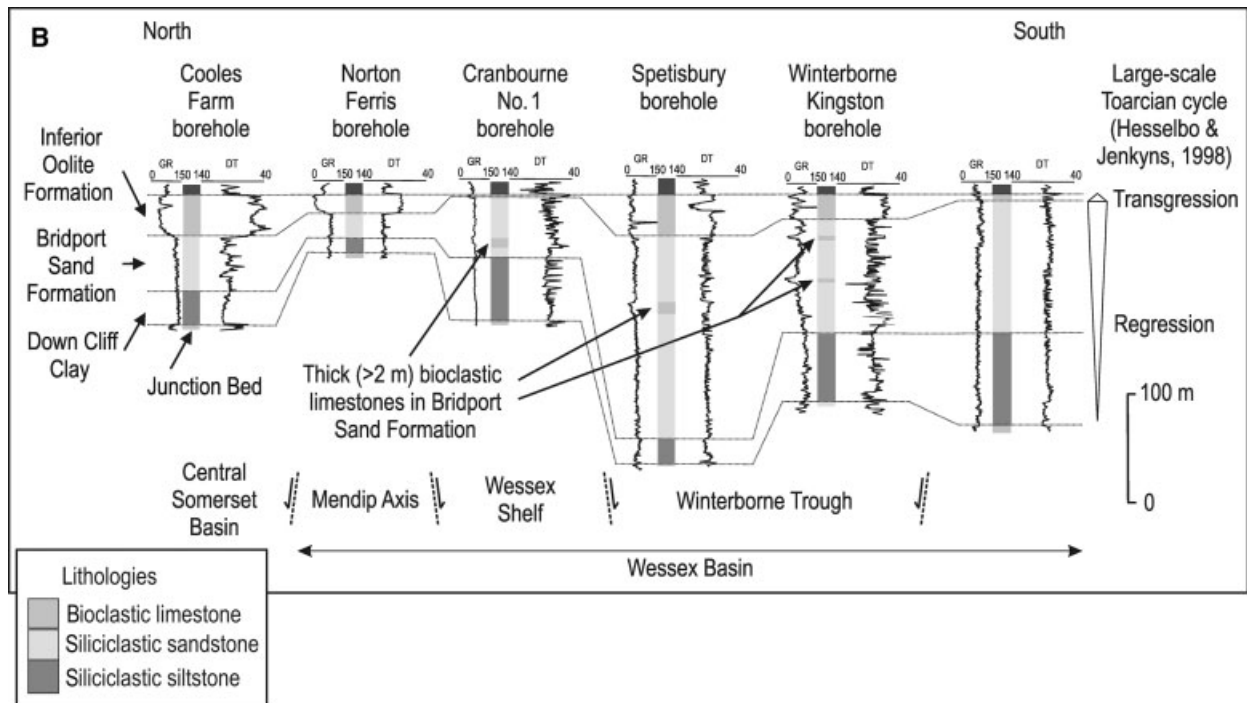


Fig. 2. Continued.

have been tied to stratal geometries and architectures observed in 3D seismic data. Regional correlation is based on key stratigraphic surfaces identified in cores and outcrops. These correlations are essentially below the resolution of biostratigraphic schemes based on either macrofossils (ammonites) or microfossils (e.g. Ainsworth *et al.*, 1998a). Vertical facies trends are repeated in several core and outcrop sections, suggesting stacked sequences. Unique correlation of these sequences is not possible in the absence of biostratigraphic constraints, and regional correlations are instead based on identifying consistent proximal-to-distal trends in lateral facies character. The resulting correlations are therefore somewhat conceptual, but they illustrate lateral variations in facies character and architecture at the scale of high-frequency sequences and their constituent systems tracts. The correlations have also been used to construct an internally consistent, high-resolution sequence stratigraphic model which can be tested against further data, when available.

GEOLOGICAL SETTING

The BSF is a lithostratigraphic unit of Toarcian (Early Jurassic) age that crops out at Bridport on the Dorset coast of southern England, UK

(Fig. 1A; Cox & Page, 2002). The unit is exposed in a narrow outcrop belt trending from south (Dorset coast) to north (Cheltenham), and has traditionally been given a variety of informal local names; Bridport Sands in Dorset, Yeovil Sands at Yeovil, Midford Sands in Bath and Cotteswold Sands in Gloucester (e.g. Davies, 1969). The BSF was deposited in a shallow epi-continental sea-way that occupied the Wessex Basin of southern England. The Wessex Basin is an east–west-oriented extensional basin filled with late Palaeozoic to Cenozoic strata (Fig. 2). The basin consists of a system of discrete depocentres and intrabasin highs defined by fault-bounded graben and half-graben (e.g. Hawkes *et al.*, 1998; Underhill & Stoneley, 1998). Fault-bounded depocentres include the Portland–South Wight Basin, Dorset Basin, Winterborne Trough, Wessex Shelf and Pewsey Basin (Fig. 2). The tectonic fabric of the Wessex Basin is dominated by east–west-trending and northwest–southeast-trending, Variscan-aged faults (Chadwick *et al.*, 1983; Day & Edwards, 1983; Lake *et al.*, 1984) that have experienced later stages of both normal and reverse reactivation. Dewey (1982) identified three main phases of crustal rifting in the area, one of which was a localized Toarcian event that succeeded an Early Triassic event and preceded a mid-Cretaceous event. As a consequence, there are significant thickness variations within the

Early Jurassic succession (e.g. Jenkyns & Senior, 1977, 1991; Whittaker, 1985; Sellwood *et al.*, 1986). Jurassic normal fault activity is interpreted as having reached a maximum during Hettangian and Sinemurian times (Chadwick, 1986) and as a result thickness variations are most marked in the lower Lias Group. However, large thickness variations also occur across east–west-trending faults in the upper Lias Group, including the BSF (Fig. 2). A particularly significant structure is the east–west-trending Mendip Axis, which coincides with the northern limit of the Pewsey Basin (and, thus, the Wessex Basin *sensu* Hawkes *et al.*, 1998; Underhill & Stoneley, 1998). The BSF and underlying DCC are absent across this structure, although a comparable succession is present further north in another depocentre (e.g. Cooles Farm borehole in Fig. 2B; Davies, 1969).

The Jurassic sedimentary fill of the Wessex Basin comprises both siliciclastic and carbonate deposits. These strata are arranged in regressive–transgressive cycles that comprise relatively deep marine mudstones and siltstones coarsening upwards into shallow-water siliciclastic sandstones in the lower, regressive part of the cycle, overlain by transgressive limestones in the upper part of the cycle (e.g. Arkell, 1933; Hesselbo & Jenkyns, 1998). The Toarcian regressive–transgressive cycle consists of the silty claystones of the DCC passing gradationally upward into the siliciclastic sandstones of the BSF, which are capped by the highly condensed limestones of the IOF (Fig. 2B). Hesselbo & Jenkyns (1998) interpreted this regressive–transgressive cycle as recording a large-scale relative sea-level cycle of *ca* 7 Ma duration bounded by major flooding

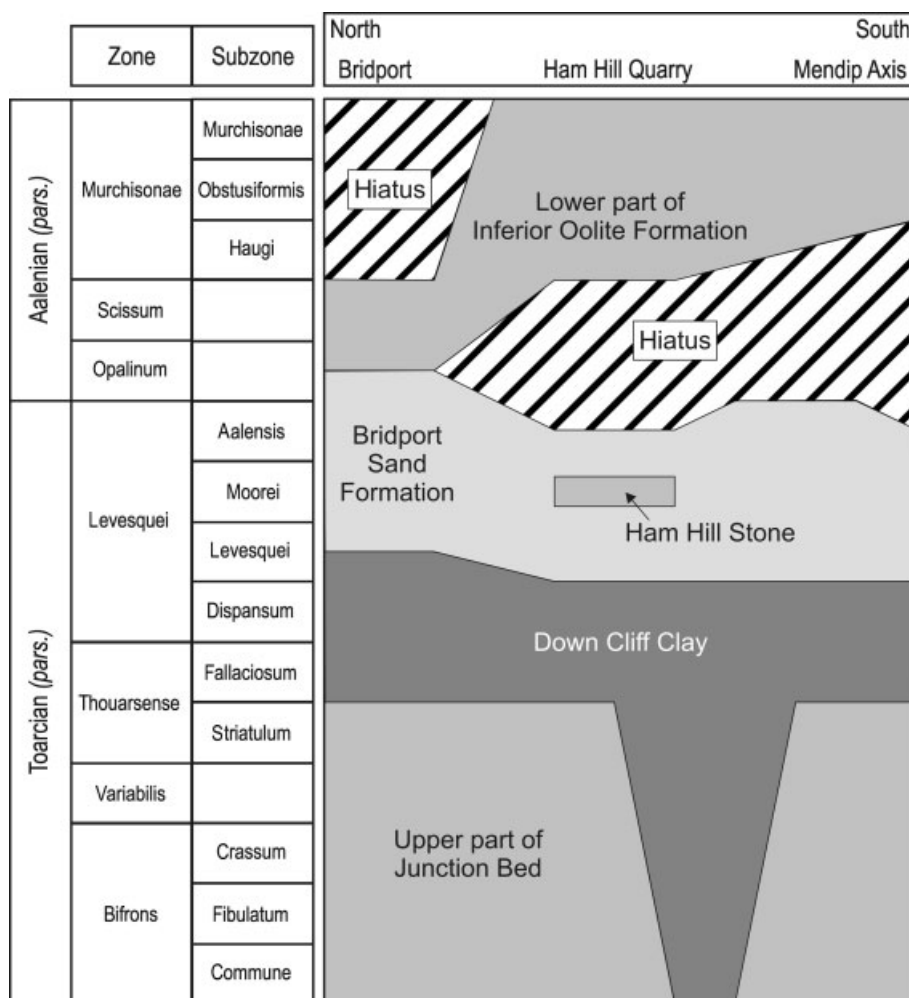


Fig. 3. Chronostratigraphic cross-section of Toarcian and early Aalenian strata within the Wessex Basin, south of the Mendip Axis (Fig. 2), illustrating the diachronous nature of the main lithostratigraphic units. Chronostratigraphy is based mainly on ammonite biozones (after Davies, 1969; Callomon & Cope, 1995; Hesselbo & Jenkyns, 1995; Cox & Page, 2002).

surfaces. Locally, there is cryptic evidence for smaller-scale cyclicity within the BSF. A thick (up to 25 m), erosively based bioclastic limestone outcropping near Yeovil locally subdivides the BSF into two successions (Ham Hill Stone; Figs 1 and 3; Buckman, 1889; Prudden, 1967; Davies, 1969). Thick (3–5 m), erosively based bioclastic limestones are also observed to bound upward-coarsening successions within the BSF in core (e.g. in the Winterbourne Kingston Borehole, Fig. 1; Knox *et al.*, 1982). Each lithostratigraphic formation in the Toarcian regressive–transgressive cycle, including the BSF, is partly diachronous and cuts across ammonite biostratigraphic zones (Fig. 3; Buckman, 1889; Arkell, 1933; Davies, 1969). On the Dorset coast, the BSF belongs to the Levesquie Zone (Toarcian) and, in its upper metre, the Opalinum Zone (Aalenian; Fig. 3; e.g. Callomon & Cope, 1995). North of the Mendip Axis, the formation was deposited in the older Thouarsense, Variabilis and Bifrons Zones (Davies, 1969). Overall, the BSF youngs towards the south, implying that the locus of sand deposition moved episodically southwards. Davies (1969) used the episodic shifting of sand depocentres to define four sand accumulations of different ages, two of which lie south of the Mendip Axis. The diachronous relationships described above imply that the BSF, DCC and more distal condensed limestones (in the underlying Junction Bed, Figs 2 and 3; e.g. Hesselbo & Jenkyns, 1995) are laterally equivalent at the scale of the Toarcian regressive–transgressive cycle. However, there is a pronounced hiatus below the IOF across much of the basin, marked locally by several missing ammonite zones (Fig. 3; e.g. Callomon & Cope, 1995; Cox & Page, 2002).

Thickness variations within the individual lithostratigraphic components of this cycle occur across east–west-trending faults (Fig. 2B), and also regionally across the Wessex Basin. For example, there is a general thinning of the BSF to the south–southeast as it passes into distal calcareous and/or ferruginous deposits (Knox *et al.*, 1982; Ainsworth *et al.*, 1998b; Hawkes *et al.*, 1998), and the DCC thins towards the south and east (Ainsworth *et al.*, 1998b). The thickness of the IOF is markedly variable across the area. For instance, in the Wytch Farm area it reaches a minimum of 1.2 m and is highly condensed compared with the northern part of the Portland-Wight Basin where it reaches 70 m (Ainsworth *et al.*, 1998b). In general, the IOF thickens towards the north. Palaeogeographies based on these gross thickness and facies trends are poorly

constrained, but show a general trend from north-west (proximal) to south-east (distal; e.g. Ainsworth *et al.*, 1998b; Hawkes *et al.*, 1998). The BSF has a marked compositional and textural uniformity across the basin, suggesting that the sediment source area did not change in character during the Toarcian (Davies, 1969). Heavy mineral assemblages suggest a metamorphic provenance, possibly a meta-igneous complex to the south-west (Boswell, 1924), consistent with thinning of the formation to the east. However, the progressive younging of the BSF towards the south means that a sediment source to the north-east cannot be ruled out (Knox *et al.*, 1982; Morton, 1982).

FACIES ASSOCIATIONS

Based on conventional facies analysis of cores and outcrops, the BSF consists of the following facies associations: (i) bioturbated siliciclastic sandstones, (ii) weakly bioturbated siliciclastic sandstones, (iii) bioclastic limestones, and (iv) oolitic ironstones. The facies associations are summarized in Table 1 and key observations and interpretations are provided below.

The bioturbated siliciclastic sandstone facies association is characteristic of the BSF at coastal exposures and in cores from the Wytch Farm Field. The facies association appears homogeneous, because physical sedimentary structures have been destroyed by intense bioturbation. In order to elucidate facies trends and interpret environments within this facies association, a combined ichnological and sedimentological scheme based on the methods of Taylor & Gawthorpe (1993) and Gowland (1996) has been used to define ichnofabrics. Parameters used to define ichnofabrics are: (i) the degree of bioturbation (bioturbation index, BI; Taylor & Goldring, 1993), (ii) the type, diversity and relative abundance of individual trace fossils, (iii) cross-cutting relationships between trace fossils, (iv) the sand and silt content, and (v) where preserved, physical sedimentary structures.

Bioturbated siliciclastic sandstones

Description

Five facies within the bioturbated siliciclastic sandstone association (DcC-t, Ss4, Ss3, Ss2 and Ss1 in Table 1) are identified using 10 pervasive ichnofabrics that are considered to reflect the conditions of ‘background’ sedimentation

Table 1. Summary of facies associations identified within the Bridport Sand Formation. BI refers to Bioturbation Index (Taylor & Goldring, 1993) and ichnofabric abbreviations are explained in Table 2.

Facies association	Facies	Description	Ichnofabrics	Interpretation
Bioturbated siliciclastic sandstones. Typically arranged in gradational, upward-coarsening facies succession comprising DcC-t (base), Ss4, Ss3, Ss2 and Ss1 (top)	DcC-t	Dark grey, highly to completely bioturbated (BI = 4–6) siltstone with thin (0.5–10 cm) beds of very fine-grained silty sandstone. Parallel lamination common in siltstones. High silt content (60–70%)	HELM, TER1, AM	Low-energy lower shoreface and offshore transition. Sandstone beds record deposition from storm events, with siltstones recording deposition from suspension during intervening fair-weather periods. Interbedding of sandstone (storm events) and siltstone (fair-weather periods) indicates deposition mostly above storm-wave base and below fair-weather-wave base. Siltstone-rich facies (DcC-t, Ss4) are assigned to offshore transition zone, and sandstone-rich facies (Ss3, Ss2, Ss1) are assigned to lower shoreface zone. Ichnofabrics indicate that benthos was less stable in the latter facies. High intensity of biogenic reworking implies low-energy shoreface and offshore transition.
	Ss4	Dark to light grey, highly to completely bioturbated (BI = 4–6), very fine-grained sandstone with siltstone partings (40–50% silt). Sandstone beds are thin (0.5–10 cm). Parallel lamination rare in siltstones	TER1, TER2, AST, P/P, R/T, AM	
	Ss3	Light grey, moderately to completely bioturbated (BI = 3–6), very fine-grained silty sandstone with irregular siltstone partings (30–40% silt). Thin (<20 cm) sandstone beds contain bioclastic debris, parallel lamination, low-angle cross-lamination, escape burrows	TER2, AST, P/P, R/T, SKOL2	
	Ss2	Light grey/yellow, poorly to completely bioturbated (BI = 2–6), fine-grained silty sandstone with irregular siltstone partings (15–30% silt). Thin (<20 cm) sandstone beds contain bioclastic debris, parallel lamination, low-angle and hummocky cross-lamination, and hummocky cross-lamination, escape burrows	P/P, R/T, ON1, SKOL1, DIP, SKOL2	
	Ss1	Light grey/yellow, sparsely to moderately bioturbated (BI = 1–3), fine-grained silty sandstone (10–15% silt). Sandstone beds up to 60 cm thick contain bioclastic debris, low-angle and hummocky cross-lamination, escape burrows	P/P, SKOL1, ON2, DIP, SKOL2	

Table 1. Continued

Facies association	Facies	Description	Ichnofabrics	Interpretation
Weakly bioturbated siliciclastic sandstones. Typically arranged in gradational, upward-coarsening facies succession comprising T3 (base), T2 and T1 (top)	T3	Variogated, thinly bedded (<15 cm) siltstones and fine-grained sandstones with thin drapes (1–2 cm) of grey clay. Sandstones are parallel and wavy laminated. Bioturbation is absent or sparse (BI = 0–1)	P/P	Protected tidal embayment? Absence of low-angle and hummocky cross-stratified event beds indicates limited storm activity and deposition in sheltered shallow-marine environment. Abundance of clay/mud drapes and bidirectional palaeocurrents indicates tidal processes were dominant. Low intensity and low diversity of bioturbation records an ecological stress (fluctuating salinities?)
	T2	Fine-grained sandstone with interbedded mudstones (20–35%). Sandstones contain low-angle cross-bedding, current ripples and mud drapes (flaser bedding). Bioturbation is absent or sparse (BI = 0–1)	P/P	
	T1	(BI = 0–1) and of low diversity Fine-grained sandstone containing current ripples with bidirectional palaeocurrents and mud drapes (10–25% mudstone). Bioturbation varies from absent to moderate (BI = 0–3)	AST, P/P	
Bioclastic limestone		Cross-bedded bioclastic limestone composed predominantly (>90%) of abraded skeletal grains (bivalves, crinoids, brachiopods, gastropods) with subordinate siliciclastic mudstones and cham- site ooids. Bioclastic limestone units are erosively based, and some infill deep (>10 m) channelized scours. Sparsely bioturbated (BI = 0–1)		Highly reworked carbonate channel-fills and/or shoals. Deposited by unidirectional currents (tides?) in channels (and shoals?) above erosion surfaces. Abraded clasts indicate significant reworking
Oolitic ironstone		Fine-grained sandstones and limestones containing a significant proportion (>15%) of iron-coated ooids, peloids and abraded bioclasts		Condensed deposits. Iron-coated ooids indicate extended physical reworking and siliciclastic sediment starvation

Table 2. Summary of ichnofabrics and their associated trace fossils identified within the Bridport Sand Formation. Ichnofabrics are divided into traces commonly associated with either the stable 'background' sedimentation (representing the equilibrium, or K-selected, endobenthos; Ekdale, 1985) or with storm-related event-beds (representing opportunistic, or r-selected, endobenthos; Ekdale, 1985). BI refers to the Bioturbation Index scheme of Taylor & Goldring (1993), which is used to describe bioturbation intensity.

Ichnofabric		Trace fossils	BI	Associated environment
Background Sedimentation (Equilibrium 'K-selected' marine endobenthos)	Helminthopsis HELM	<i>Helminthopsis</i> , small <i>Teichichnus</i> , <i>Chondrites</i> , <i>Planolites</i> , <i>Anconichnus</i> .	5–6	
	Terebellina 1 TER1	<i>Terebellina</i> , <i>Helminthopsis</i> , <i>Zoophycus</i> , <i>Asterosoma</i> , <i>Chondrites</i> , <i>Planolites</i> , small <i>Teichichnus</i> .	5–6	
	Terebellina 2 TER2	<i>Terebellina</i> , small <i>Teichichnus</i> , <i>Anconichnus</i> , large <i>Asterosoma</i> , <i>Chondrites</i> , <i>Planolites</i> , <i>Palaeophycus</i> , small <i>Helminthopsis</i> , small <i>Rhizocorallium</i> .	4–6	
	Asterosoma AST	Large <i>Asterosoma</i> , <i>Anconichnus</i> , small <i>Teichichnus</i> , <i>Planolites</i> , <i>Palaeophycus</i> , <i>Phoebichnus</i> , <i>Thalassinoides</i> , <i>Chondrites</i> , small <i>Helminthopsis</i> , <i>Rhizocorallium</i> .	4–6	
	Planolites/ Palaeophycus P/P	<i>Planolites</i> , <i>Palaeophycus</i> , <i>Phoebichnus</i> , <i>Anconichnus</i> , <i>Arenicolites</i> , <i>Thalassinoides</i> , small <i>Diplocraterion</i> .	4–6	
	Rhizocorallium/ Teichichnus R/T	Large <i>Rhizocorallium</i> , large <i>Teichichnus</i> , <i>Planolites</i> , <i>Arenicolites</i> , <i>Anconichnus</i> , <i>Palaeophycus</i> , <i>Skolithos</i> , small <i>Asterosoma</i> , <i>Thalassinoides</i> . Occasional small <i>Diplocraterion</i> , <i>Ophiomorpha</i> .	2–6	
	Ophiomorpha Nodosa 1 ON1	<i>Ophiomorpha nodosa</i> , <i>Skolithos</i> , <i>Diplocraterion</i> , <i>Planolites</i> , <i>Phoebichnus</i> , <i>Rhizocorallium</i> .	2–4	
	Skolithos 1 SKOL1	<i>Skolithos</i> , <i>Palaeophycus</i> , <i>Planolites</i> , <i>Anconichnus</i> , <i>Thalassinoides</i> .	2–6	
	Ophiomorpha Nodosa 2 ON2	<i>Ophiomorpha nodosa</i> . Occasional <i>Skolithos</i> , <i>Palaeophycus</i> .	1–3	
Diplocraterion DIP	<i>Diplocraterion</i> .	2–6		
Event Beds (Opportunistic 'r-selected' marine endobenthos)	Anconichnus mottling AM	<i>Anconichnus horizontalis</i> .	5–6	Distal storm event beds in offshore transition setting.
	Skolithos 2 SKOL2	<i>Skolithos</i> , <i>Arenicolites</i> , <i>Diplocraterion</i> , <i>Ophiomorpha</i> , <i>Palaeophycus</i> , <i>Phoebichnus</i> , escape structures.	5–6	Sharp-based, bioclastic-rich storm event beds common in shoreface settings.
	Thalassinoides THAL	<i>Thalassinoides</i> and <i>Diplocraterion</i> crosscutting all the fabrics described above.	5–6	<i>Glossifungites</i> ichnofacies. Hiatal firmground surface.

(Table 2). A further three ichnofabrics occur within event beds. Facies DcC-t occurs at the transition from the BSF into the underlying DCC, and is characterized by a high silt content (60–70%), parallel lamination and ichnofabrics exhibiting intense to complete bioturbation with the following trace fossils: *Helminthopsis*, *Tere-*

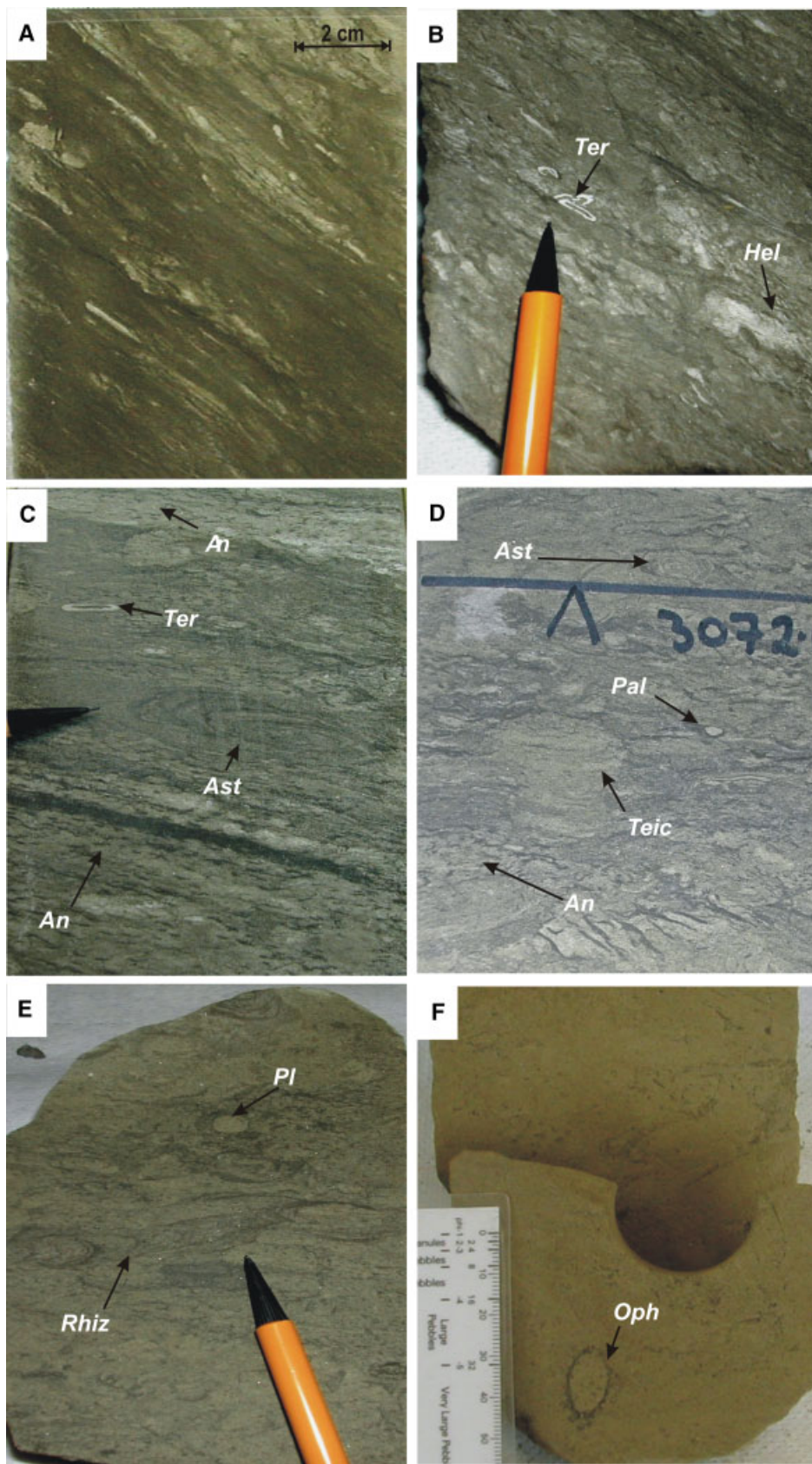
bellina (*sensu lato*; see Miller, 1995 for discussion of ichnogenus terminology), *Chondrites* and *Zoophycos* (Fig. 4B). Typically, deposits of facies DcC-t are overlain by deposits of facies Ss4. Facies Ss4 is silt-rich (40–50% silt) and contains ichnofabrics that exhibit high to complete bioturbation with *Terebellina*, *Chondrites*,

Asterosoma and *Anconichnus* (Fig. 4C). Facies DcC-t and Ss4 contain thin (<10 cm) relict beds of cleaner sand that contain an abundance of the trace fossil *Anconichnus* and are calcite-cemented (Fig. 5A). At the coastal outcrops (Bridport, Fig. 1A), a single surface characterized by large, near-sinusoidal undulations (29–42 m in wavelength, 0.95–1.8 m in height; Pickering, 1995) occurs within deposits of facies Ss4 (Davies, 1967; Hesselbo & Jenkyns, 1995; Pickering, 1995). The surface erodes into underlying beds, and is overlain by laminae that drape the topography of the surface and lack cross-stratification (Davies, 1967; Hesselbo & Jenkyns, 1995; Pickering, 1995). Deposits of facies Ss4 are overlain by those of facies Ss3, which contains less silt (30–40%) and ichnofabrics dominated by *Teichichnus*, *Asterosoma* and *Planolites* (Fig. 4D). Facies Ss2, which typically gradationally overlies facies Ss3, is sand-rich (15–30% silt) and contains ichnofabrics that exhibit low to complete bioturbation with *Teichichnus*, *Planolites*, *Palaeophycus* and *Rhizocorallium* (Fig. 4E). The lower parts of thin (<20 cm), fine-grained sandstone beds containing parallel lamination, low-angle and hummocky cross-lamination are preserved in both facies Ss3 and Ss2. Deposits of facies Ss1 are rare and, where present, they gradationally overlie deposits of facies Ss2. Facies Ss1 is sand-rich (10–15% silt) and contains ichnofabrics with sparse to high bioturbation with *Skolithos*, *Diplocraterion* and *Ophiomorpha* (Fig. 4F). In facies Ss1, parallel lamination and low-angle cross-lamination occur in the lower part of fine-grained sandstone beds up to 60 cm thick (Fig. 5B). In facies Ss3 to Ss1, relatively thick (up to 60 cm) fine-grained sandstone beds, including those containing preserved lamination, are typically calcite-cemented and contain vertical trace fossils such as *Skolithos*, *Diplocraterion* and escape burrows. Many of these beds also contain abundant bioclastic material, including articulated bivalves (Fig. 5C), but more commonly fragmented shell debris (Fig. 5D).

Interpretation

Overall, the trace fossil assemblages of this facies association represent Seilacher's (1967) Cruziana and Skolithos ichnofacies, implying a nearshore environment. All facies contain the preserved remnants of event beds. Event beds are normally graded, have sharp or erosive bases, and contain bioclastic lags and low-angle

or hummocky cross-stratification (Fig. 5). These characteristics record deposition from episodic waning flows, most likely from oscillatory storm-wave currents (Dott & Bourgeois, 1982; Bryant *et al.*, 1988). Trace fossil assemblages indicate rapid colonization of these event beds by opportunistic feeders (Bryant *et al.*, 1988; Pemberton & MacEachern, 1997). Bioclastic lags may record transport of shells from shallower water by storm currents and/or reworking and winnowing of bioclasts on the seafloor by continued storm activity. Event beds therefore record deposition above storm-wave base, while the high silt content and pervasive bioturbation indicate that sediment was not winnowed and reworked by fairweather waves. Silt is interpreted as having been deposited during fairweather periods ('background' sedimentation), but was then redistributed by pervasive bioturbation (Bryant *et al.*, 1988). Siltier facies (e.g. DcC-t) are characterized by a greater intensity of bioturbation and trace fossils that record predominantly horizontal grazing. Sandier facies (e.g. Ss1) are characterized by less intense bioturbation and trace fossils that record mainly vertical suspension feeding. In combination, these characteristics suggest that siltier facies record deeper water deposition, and each successive facies records deposition in progressively shallower water conditions that were increasingly hostile to marine endobenthos (Fig. 6). However, all facies lack evidence for fair-weather wave action, and are thus assigned to lower shoreface and offshore zones. Individual facies are interpreted as representing the following environments (using the shoreface terminology of Van Wagoner *et al.*, 1990 and Hampson & Storms, 2003): distal offshore transition/offshore (facies DcC-t), proximal offshore transition (facies Ss4), distal lower shoreface (facies Ss3), proximal/distal lower shoreface (facies Ss2) and proximal lower shoreface (facies Ss1). The specific environments allocated to each facies are based on published ichnological models for similar deposits in which terminology reflects water depth with respect to storm-wave base and fairweather-wave base, not the interpreted physiography of the shoreline-shelf profile (e.g. Pemberton *et al.*, 1992; Taylor & Goldring, 1993; Gowland, 1996; Martin & Pollard, 1996). The large, near-sinusoidal undulations documented in facies Ss4 at the coastal outcrops (Bridport, Fig. 1A) are interpreted as relict, large (sandwave-scale), near-symmetrical bedforms. The draped character



of overlying laminae and the absence of cross-stratification suggests bedform aggradation by suspension fall-out. These enigmatic structures have been interpreted as the product of storm-generated standing waves (Pickering, 1995), which is consistent with their facies context, possibly at the toe of a slope (Hesselbo & Jenkyns, 1995).

Origin of calcite cement

Detailed analysis of calcite-cemented beds in the bioturbated siliciclastic sandstone association reveals that these beds have undergone little compaction, and that cementation therefore took place predominantly during early diagenesis (Davies, 1967; Knox *et al.*, 1982; Bjørkum & Walderhaug, 1990, 1993). The cement comprises ferroan low-Mg calcite spar, and petrographic data suggests that it was mainly locally derived from the dissolution of aragonitic bioclasts (Knox *et al.*, 1982; Storey, 1990; Bjørkum & Walderhaug, 1993). Early precipitation of cement is interpreted as having occurred preferentially in beds marked by sharp contrasts in porosity or permeability (e.g. coarser-grained and better-sorted event beds enclosed in intensely bioturbated 'background' deposits; Knox *et al.*, 1982) and in the vicinity of laterally continuous lags of bioclastic debris (Bjørkum & Walderhaug, 1990; Storey, 1990). These findings are consistent with the interpretation of calcite-cemented sandstone beds as storm-event beds rich in bioclastic debris.

Wireline-log character

It is not possible to robustly recognize the subtle character of the individual facies described above on wireline logs. However, decreases and increases in silt content within successions of the facies association, reflecting shallowing and deepening

respectively, can be detected using gamma-ray and neutron-density logs. Calcite-cemented horizons can be robustly identified in sonic, micro-resistivity and density/neutron logs, but are most clearly expressed as thin intervals of high velocity in sonic logs (e.g. Knox *et al.*, 1982; Bryant *et al.*, 1988). The abundance of such cemented beds in vertical successions of the bioturbated siliciclastic sandstone facies association produces a highly serrate log character.

Weakly bioturbated siliciclastic sandstones

Description

The weakly bioturbated sandstone facies association has been identified in inland exposures only (e.g. Ham Hill Quarry, Fig. 1; Davies, 1969; Hounslow, 1987). The association comprises three facies (Table 1) which have gradational boundaries and are stacked vertically into upward-coarsening successions of interbedded siltstones and sandstones (facies T3), overlain by flaser-bedded sandstones (facies T2) and ripple-laminated, weakly bioturbated sandstones (facies T1). Facies T3 comprises thin (<15 cm) beds of parallel-laminated, variegated siltstones and fine-grained sandstones interbedded with thin (1–2 cm), structureless grey clay beds (Fig. 7A). Sedimentary structures and bioturbation are rare, but include clay-draped wavy bedding and *Planolites*(?) burrows. Where this facies locally overlies bioclastic limestone deposits (see below), it contains thick (40 cm), sharp-based beds of tabular cross-bedded, bioclastic limestone. Palynological analysis of the clay-rich siltstone intervals in facies T3 indicates shallow-water winnowing or clastic dilution relative to siltstones in the DCC (see *Appendix*). Facies T2 consists of flaser bedded, fine-grained sandstone. Bioturbation is sparse

Fig. 4. Core photographs of the bioturbated siliciclastic sandstone facies association, illustrating key traces and pervasive ichnofabrics used in ichnofabric analysis (Tables 1 and 2). Notes that the cores in panels A–C were taken from wells deviated at a high angle to bedding. (A) The Down Cliff Clay has a high silt content (>70%) and contains sparse bioturbation (BI = 0–1) and parallel lamination, interpreted as recording predominantly deposition from suspension in an offshore setting. (B) Deposits of facies DcC-t and Ss4 containing *Terebellina* (*Ter*), *Zoophycos*, *Helminthopsis* (*Hel*) and *Chondrites*. (C) Intensely bioturbated (BI = 4–6) deposits of facies Ss4 contain large *Asterosoma* (*Ast*) and *Terebellina* traces, and reflect 'background' sedimentation. The lighter-coloured sand-rich units at the base and top of the photograph contain event-bed colonization by opportunistic *Anconichnus* (*An*). (D) Intensely bioturbated (BI = 4–6) deposits of facies Ss3 contain abundant *Teichichnus* (*Teic*), *Palaeophycos* (*Pal*) and small *Asterosoma*. (E) Deposits of facies Ss2 have a relatively low silt content (<30%). Trace fossils are predominantly horizontal and record grazing behaviours (e.g. *Rhizocorallium*, *Rhiz* and *Planolites*, *Pl*). (F) Poorly bioturbated (BI = 0–3) deposits of facies Ss1 with a low silt content (<15%). Traces include vertical *Ophiomorpha* (*Oph*), which records suspension feeding behaviour. The change in behaviour from horizontal grazing in facies Ss2 to vertical suspension feeding of endobenthos in facies Ss1 reflects higher-energy conditions.

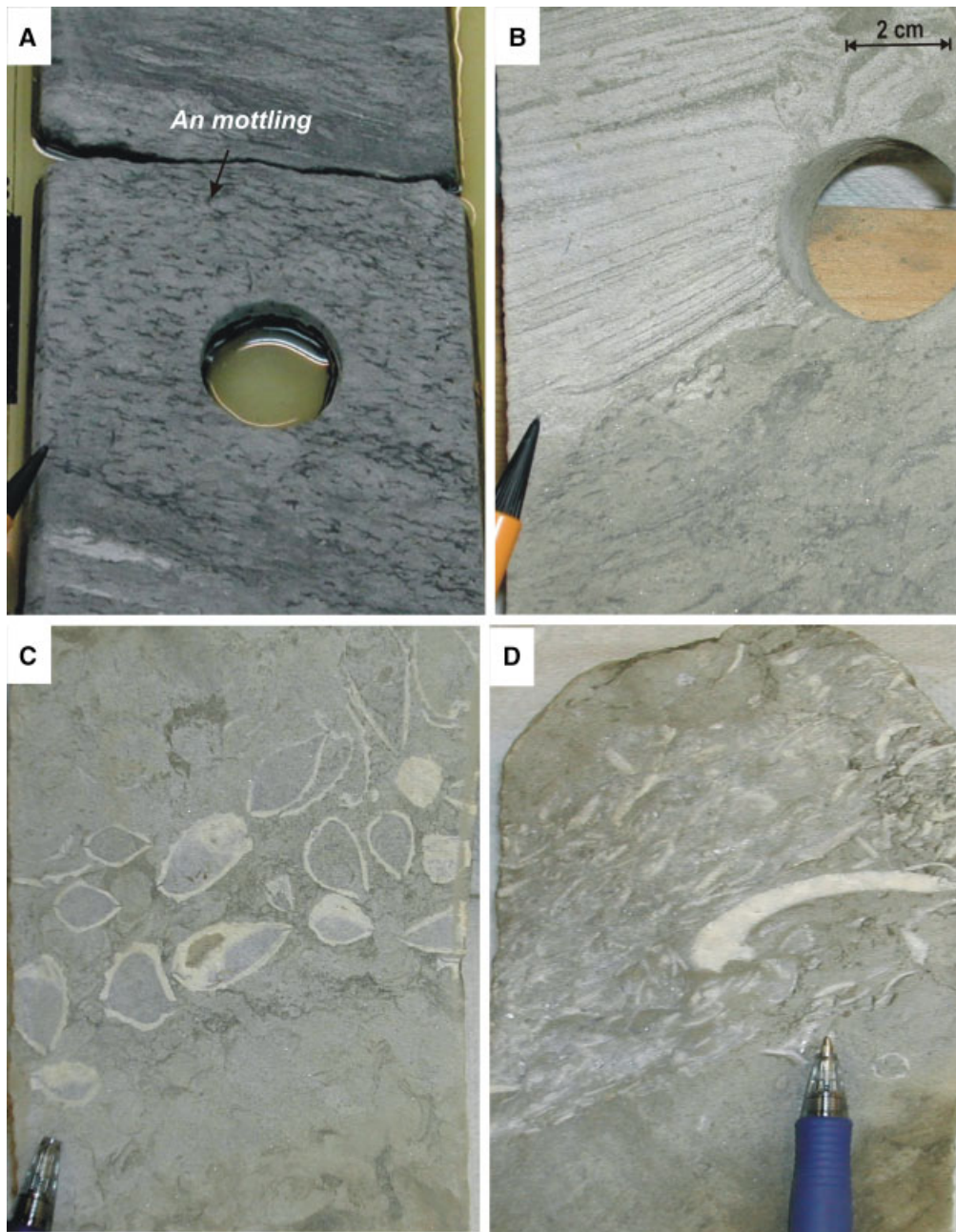


Fig. 5. Types of event-bed deposition recorded in core. (A) The opportunistic trace fossil *Anconichnus* colonized rapidly emplaced sand-rich event beds producing a characteristic mottled fabric within facies DcC-t (Tables 1 and 2). This fabric is often the only indicator of original bedding. (B) A sharp-based, laminated sandstone bed, interpreted as a high-energy event bed, which sharply overlies intensely bioturbated deposits (facies Ss3), representing 'background' sedimentation. Sparse bioturbation within the event bed reflects its rapid rate of deposition, which inhibited infaunal reworking and allowed preservation of primary sedimentary structures. (C) A lag of articulated, randomly orientated brachiopod shells at the base of a calcite-cemented sandstone bed within facies Ss2. Pseudomorphs of shells can be seen above and below this lag indicating dissolution of carbonate shell material prior to calcite precipitation during early diagenesis. (D) Calcite-cemented sandstone beds are also associated with disarticulated shells and bioclast shards, which are aligned along a weak lamination fabric (facies Ss2).

(monospecific *Planolites*) and sedimentary structures include small-scale, mud-draped low-angle cross bedding and current ripples. Facies T1 consists of fine-grained sandstones with well-

preserved current ripple trough cross-lamination arranged in cosets with bi-directional palaeocurrents (Fig. 7B; also palaeocurrent rose diagram for 10.0–12.5 m in Fig. 8). Bioturbation is

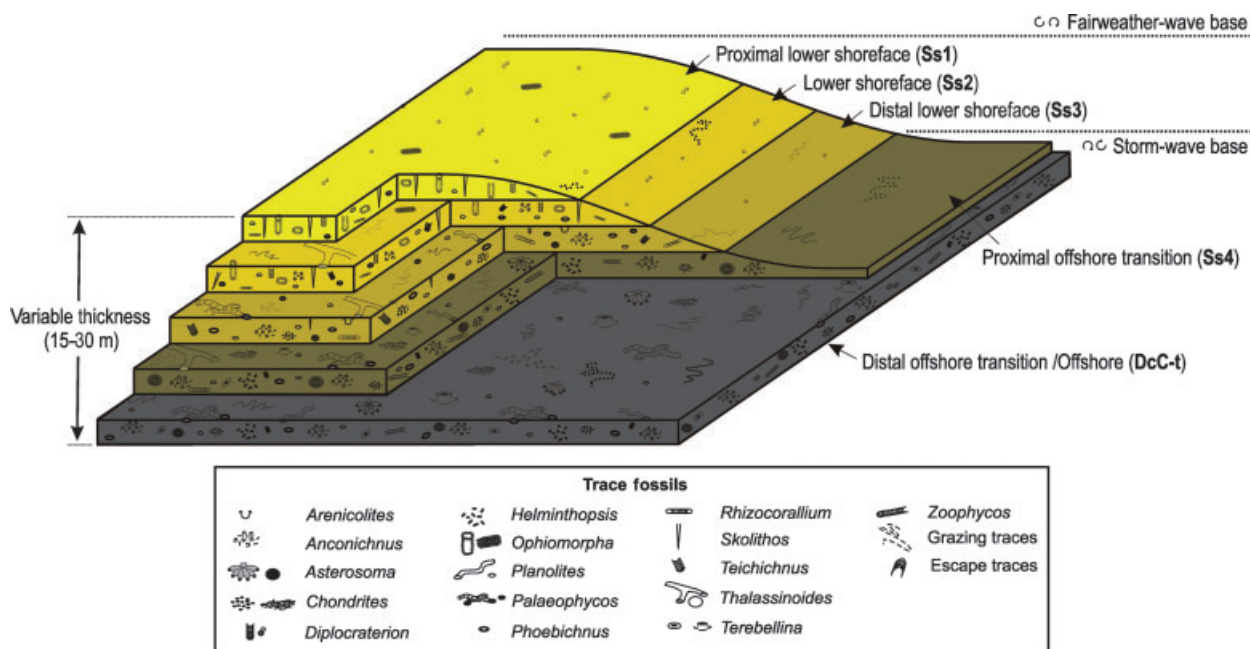


Fig. 6. Facies model of the bioturbated sandstone association, showing trace fossil assemblages and inferred palaeobathymetry. Each facies is represented by characteristic ichnofabric assemblages (Table 2), which are used to interpret the environment of deposition within a shoreface to offshore setting.

sporadic, and varies from absent to moderate in intensity. Locally, facies T1 is gradationally overlain by deposits of the bioturbated siliciclastic sandstone facies association (Fig. 8).

Interpretation

Facies T3, T2 and T1 are interpreted as recording deposition from tidal currents, with bi-directional palaeocurrents in current-rippled sandstones indicating opposing tidal currents (e.g. ebb and flood tides) and clay drapes and flasers recording deposition from suspension during slack water conditions. The clay-rich character of facies T3 implies low-energy conditions, whereas the decrease in clay content and concomitant increase in cross-laminated sandstone in facies T2 and T1 indicate higher energy deposition. The scarcity of bioturbation in all three facies indicates a significant change of environment compared with the bioturbated sandstone facies association described above. The low intensity and generally low diversity of bioturbation is interpreted as reflecting an ecological stress, consistent with mixed salinities in a tidal environment (e.g. Bromley, 1996), rather than physical reworking in a relatively high-energy environment (e.g. the bar environment of Davies, 1969). However, the increased intensity of bioturbation in facies T1 and its gradational contact with the bioturbated sandstone facies association are interpreted as reflecting a transition to

normal marine conditions. The absence of storm- and/or wave-generated structures (e.g. hummocky cross-stratification, swash-backwash lamination) implies deposition in a protected environment in which tides were the dominant process, possibly in a tidal embayment. The laterally discontinuous character of inland exposures precludes more detailed interpretation of the environmental and palaeogeographic context of this facies association.

Bioclastic limestone

Description

Deposits of the bioclastic limestone facies association have been observed both in core and at outcrop, where they occur intercalated within the siliciclastic sandstones (described above) of the BSF. Similar deposits also occur locally in the lower few metres of the overlying IOF (e.g. in cores from the Wytch Farm Field).

In core, this facies association occurs as sharp-based units of varying thickness (0.7–4.5 m) composed predominantly (>90%) of bioclastic debris (Knox *et al.*, 1982). The principal bioclastic constituents are fragmented bivalves, crinoid ossicles, brachiopods and gastropods. Many skeletal grains have abraded and/or bored rims (Knox *et al.*, 1982). In addition to the skeletal grains, entire or broken chamosite ooids

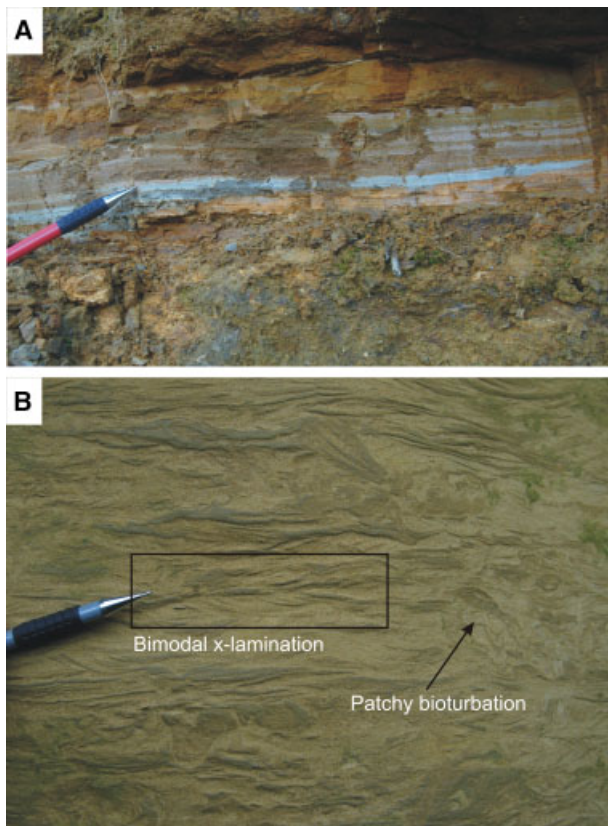


Fig. 7. Photographs of the weakly bioturbated siliciclastic sandstone at outcrop. (A) Deposits of facies T3 contain clay beds 1–2 cm thick within orange/brown siltstones and fine-grained sandstones, reflecting deposition in a low-energy environment. (B) Sandstones of facies T1 contain current ripple cross-lamination exhibiting opposed palaeocurrent directions and flaser bedding. Bioturbation is sparse and patchy.

are common, although chamosite is locally replaced by phosphate (Knox *et al.*, 1982). Within thicker units (>2 m), the limestone contains cross-bed sets of variable thickness (0.05–1 m) and orientation (e.g. Knox *et al.*, 1982). Cross-bed foresets are steeply dipping (up to 20°; Knox *et al.*, 1982) and are composed of rounded, aligned bioclast fragments. Thin horizontal beds (<5 cm) of similar character also occur, and are intercalated with thin (<1 cm), clay-rich mudstones. Thin units (<2 m) of the bioclastic limestone contain isolated, thin (<0.2 m) cross-bedded sets and consist of reworked bioclastic material alternating with green-grey mudstone and sandstone interbeds.

At outcrop, the facies association is represented by a thick (up to 27 m), cross-bedded, bioclastic limestone locally known as the Ham Hill Stone (Buckman, 1889; Prudden, 1967; Davies, 1969). The Ham Hill Stone forms an elongate body 10 km long, 3–4 km wide and oriented approxi-

mately north–south (Davies, 1969). Cross-bedding in the limestone indicates palaeocurrents to the north-east (Fig. 8; Davies, 1969). In detail, the Ham Hill Stone succession contains two erosively based bioclastic limestone units, a thicker (>10 m) lower unit and a thinner (<2 m) ‘flaggy’ upper unit, separated by siliciclastic sandstones and siltstones (facies T1–T3, S1–S4; Fig. 8). Each limestone unit has an erosive base lined by a lag of large (>30 cm) clasts of cemented siliciclastic sandstone (Fig. 8; Davies, 1969), which are described in more detail below.

Interpretation

The pervasive, cross-bedded character of the bioclastic limestones indicates deposition by dune-scale bedforms migrating in response to unidirectional currents. The abundance of diverse, shallow-marine bioclasts implies deposition in a shallow-water, fully marine environment(s). The abundance of high-angle cross-beds and the absence of storm- and/or wave-generated structures may record deposition above fair-weather wave base by tidal and/or wave-generated longshore currents. The erosive bases and limited lateral extent of the limestones documented at outcrop implies deposition within deeply eroded channels (Davies, 1969). Davies (1969) interpreted the Ham Hill Stone as the deposits of tidal channels, although there is no direct evidence of tidal processes (e.g. paired mud drapes, bi-directional palaeocurrents). The bioclastic limestone units observed in core are sharp-based, similar to the Ham Hill Stone, but are thinner (<4.5 m) and their geometries are poorly defined. These cross-bedded units may record deposition in a variety of shallow-marine environments: shelfal shoals, barred upper shoreface and/or channels.

Wireline-log character

Bioclastic limestone units can be identified in sonic, micro-resistivity and density/neutron logs, but are most clearly expressed as intervals of high velocity in sonic logs (e.g. Knox *et al.*, 1982). However, the limestone units have a near-identical wireline-log response to calcite-cemented sandstone beds within the bioturbated sandstone facies association, and can only be distinguished from the latter in cases where they have markedly greater thickness (>2 m) and from their sparser distribution in vertical section (>10 m vertical spacing). Robust distinction between bioclastic limestones and calcite-cemented sandstone beds relies on core data,

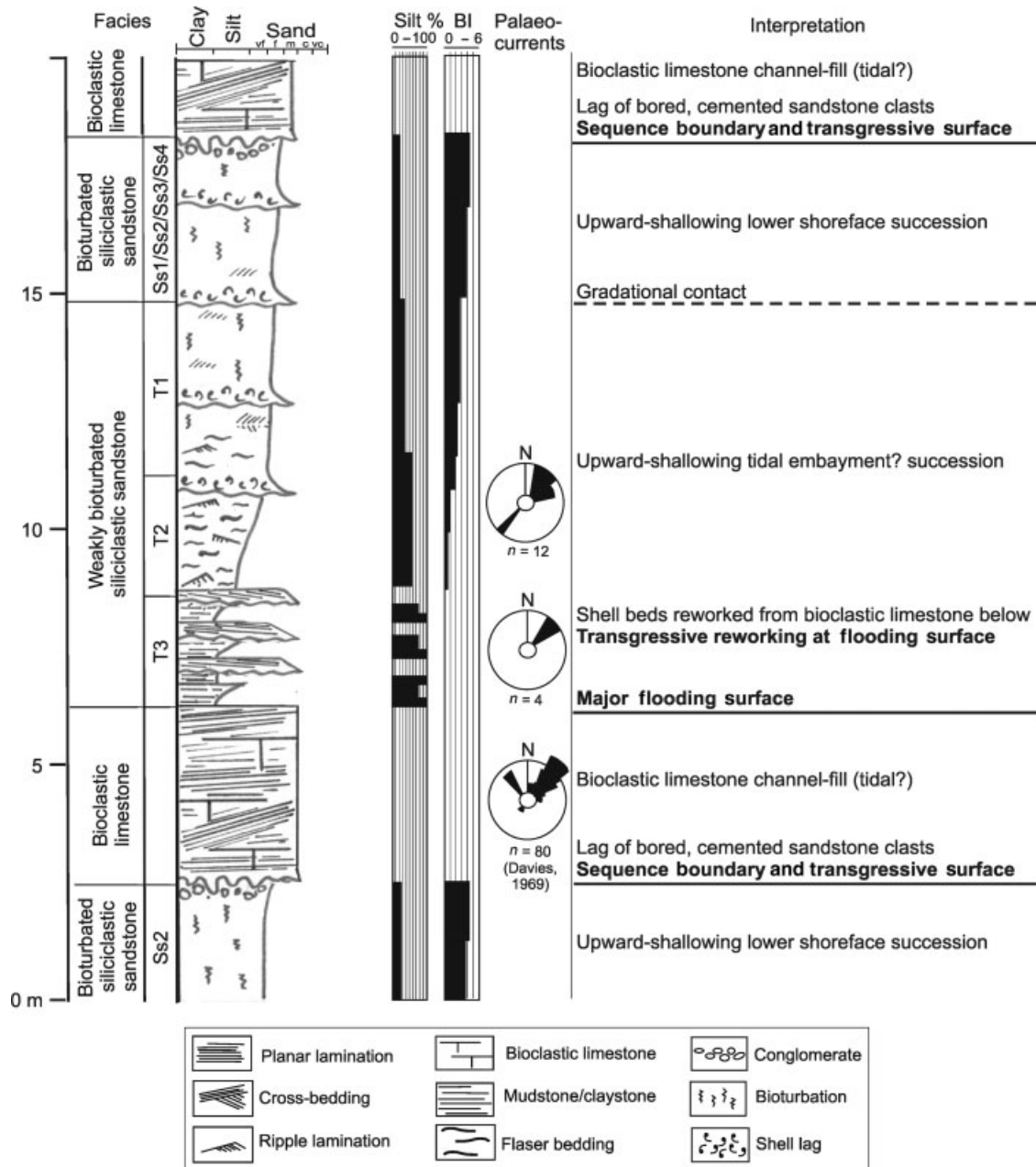


Fig. 8. Composite log illustrating the succession of the Ham Hill Stone at Ham Hill Quarry (Fig. 1A; UK Ordnance Survey grid reference: ST 470 160). Palaeocurrents in the bioclastic limestone units and weakly bioturbated siliciclastic sandstones and siltstones (facies T3 and T2) trend dominantly towards the north-east (Davies, 1969). Siliciclastic deposits between the lower and upper limestone units record an overall upward-coarsening trend, and are interpreted as recording an upward transition from protected tidal embayment to fully marine, lower-shoreface environment.

particularly where bioclastic limestones are thin (<2 m).

Oolitic ironstone

Description

The oolitic ironstone facies association has been recorded in core and wireline-log data (e.g. the

'ferruginous facies' of Ainsworth *et al.*, 1998b), for example in thin (<6 m) units within the cores from the Winterborne Kingston and the Marchwood boreholes (Fig. 1), but is not documented at outcrop. The facies association comprises ferruginous, fine-grained sandstones and limestones that contain a significant proportion (>15%) of iron-coated grains and therefore can

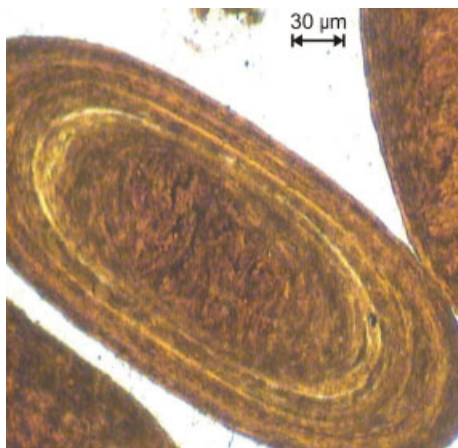


Fig. 9. Photomicrograph of ferruginous ooid from the Marchwood borehole (Fig. 1A). Iron-coated concentric laminae are well preserved internally, indicating primary deposition within an iron-enriched, energetic, shallow-marine setting starved of siliciclastic sediment.

be described as ironstones (Adams *et al.*, 1984). In thin section (Fig. 9), the association contains well-rounded ferruginous allochems of ooids, peloids and abraded bioclastic debris set within a matrix of sub-angular quartz, mica, feldspar and blocky calcite grains that lack iron-mineral coatings. The matrix may also comprise structureless green mudstone, and contain rare ammonite and belemnite fragments (e.g. the ‘ammonite bed’ of Knox *et al.*, 1982). Ferruginous ooids and peloids have commonly been completely altered to goethite and/or limonite, or replaced by phosphate (e.g. Knox *et al.*, 1982), but several ooids contain concentric layers of original berthierine or chamosite (Fig. 9). Iron ooids and iron-stained, fragmented bioclastic debris also occur within some bioclastic limestone units observed in core. Oolitic ironstones are more common in the eastern part of the study area (e.g. Ainsworth *et al.*, 1998b). For example, they comprise *ca* 35% of the BSF succession cored in the Marchwood borehole (Fig. 1).

Interpretation

The development of primary iron-coated (e.g. chamositic) ooids requires extended physical reworking, a relatively high supply of iron, and siliciclastic sediment starvation to allow iron enrichment (Young, 1989). Iron may have been supplied by either a marine or reworked pedogenic source. These conditions suggest that the oolitic ironstones represent condensed deposition. However, the dispersal of ferruginous

allochems within a matrix of siliciclastic and/or carbonate sediment suggests that condensed deposits were probably subsequently reworked. This facies association is interpreted as representing a distal component of the BSF (e.g. Ainsworth *et al.*, 1998b), and its increasing abundance towards the east of the study area supports the notion that the siliciclastic depositional system(s) of the BSF prograded towards the east.

Wireline-log character

The oolitic ironstones exhibit lower gamma-ray and higher sonic velocity responses than the bioturbated sandstone facies association that forms most of the BSF (Ainsworth *et al.*, 1998b), which allows them to be robustly identified in wireline-log data (e.g. in the Winterborne Kingston borehole, Knox *et al.*, 1982).

FACIES SUCCESSIONS, KEY STRATIGRAPHIC SURFACES AND STRATIGRAPHIC ARCHITECTURE

Using the facies associations described above, core and outcrop sections have been subdivided into successions of genetically related facies, bounded by key stratigraphic surfaces. Key stratigraphic surfaces are interpreted using their geometry, the sense of facies dislocation across them (i.e. basinward or landward facies shift), and the character of any associated lag deposits. Key stratigraphic surfaces have also been assigned to a hierarchy, according to the magnitude of facies dislocation interpreted across them. Where possible, the internal architecture of facies successions is described using 3D seismic and outcrop data.

Major and minor flooding surfaces within bioturbated siliciclastic sandstones

Successions of the bioturbated siliciclastic sandstone facies association are interpreted as recording an overall shallowing upward from offshore transition zone to middle shoreface (between facies DcC-t and Ss1; Fig. 6). However, there is not a gradual transition between facies representing deposition in progressively shallower water environments. Instead, the bioturbated siliciclastic sandstones contain surfaces across which there is an abrupt vertical change from underlying proximal to overlying distal facies (e.g. from facies Ss1 to Ss4 at 968 m in Fig. 10). Based on their characteristic facies dislocation, which

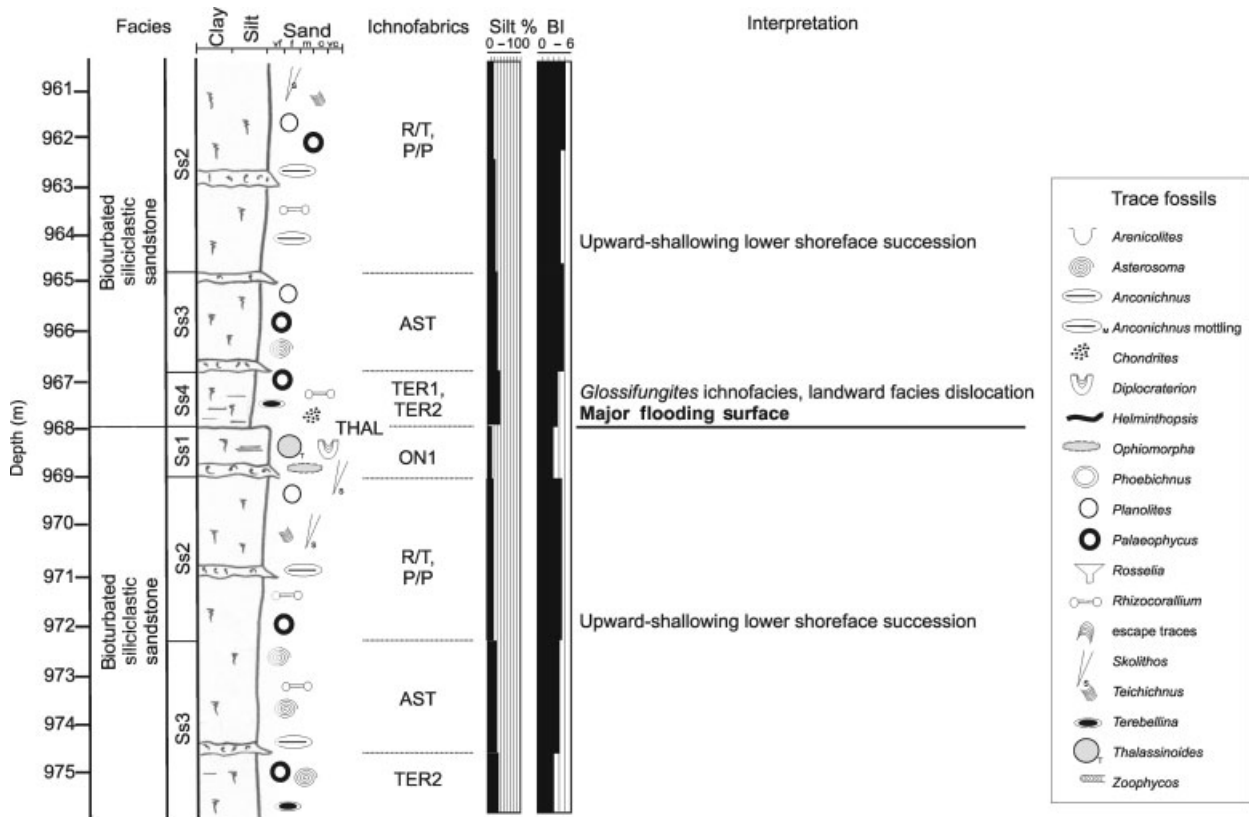


Fig. 10. Section of core log illustrating the facies juxtaposition across a major flooding surface that separates two upward-shallowing successions of bioturbated siliciclastic sandstones (well G03, Wytch Farm Field; Fig. 1B). The major flooding surface is characterized by large landward facies dislocation (facies Ss4 juxtaposed above facies Ss1 at 968 m). Key to sedimentary structures as for Fig. 8.

records an increase in water depth, the surfaces are interpreted as flooding surfaces. Two types of flooding surface are recognized, based on the magnitude of facies dislocation across the surface.

Major flooding surfaces are marked by vertical dislocations of three or more facies belts (e.g. from facies Ss1 to Ss4 at 968 m in Fig. 10), which is interpreted as representing an increased water depth of at least 10 m (cf. Fig. 6). The surfaces may also be associated with unlined *Thalassinoides* burrows, which are interpreted as constituting a firmground, *Glossifungites* ichnofacies (MacEachern *et al.*, 1992; e.g. at 968 m in Fig. 10). This interpretation implies that the surfaces were exhumed by transgressive erosion. Major flooding surfaces bound thick (10–20 m) successions that contain upward-shallowing facies trends internally, which most likely represent parasequences (e.g. Van Wagoner *et al.*, 1990). A typical core through the BSF contains 1–3 successions of this type, which are characterized by an upward decrease in silt content inferred from gamma-ray and neutron-density log trends (i.e. ‘cleaning-

upward’ log trend). Where overlain by siltstone-dominated facies, major flooding surfaces also coincide with vertical breaks in reservoir pressure recorded by repeat formation test data in the Wytch Farm Field. These pressure breaks imply that siltstones overlying major flooding surfaces form laterally extensive permeability barriers that prevent pressure communication between overlying and underlying successions over the time-scale of oil production.

Minor flooding surfaces are represented by more subtle facies dislocations, generally of a single facies belt (e.g. from facies Ss3 to Ss4 at 940.2 and 938.7 m in Fig. 11). The surfaces are interpreted as representing metre-scale increases in water depth (cf. Fig. 6), although they may also be the result of minor variations in wave climate and/or sediment supply (e.g. Storms & Hampson, 2005). Typically these surfaces bound thin (<5 m) coarsening- and fining-upward packages of beds (e.g. the bedsets of Van Wagoner *et al.*, 1990) that can be resolved in core, but not in well-logs. Minor flooding surfaces are superimposed on

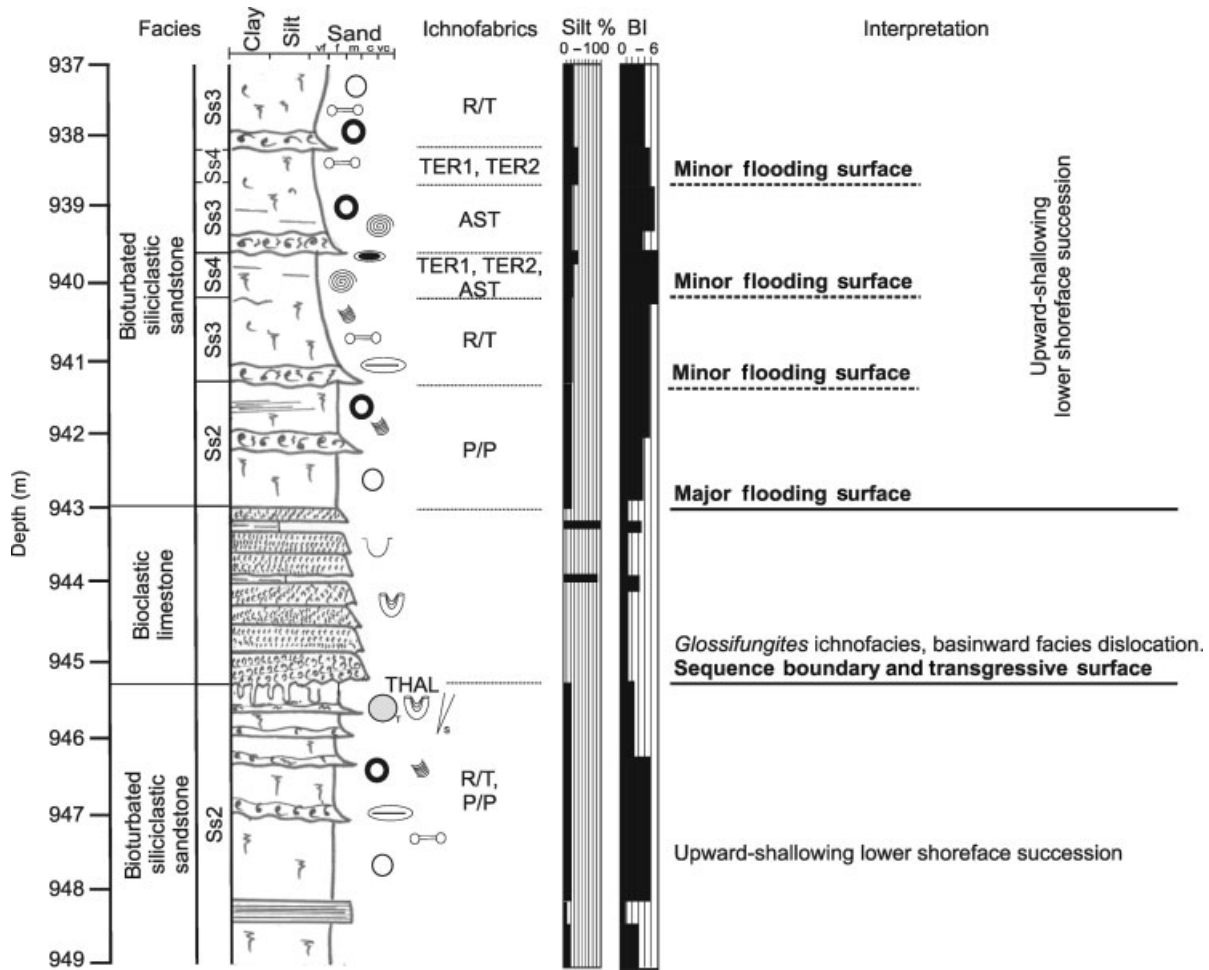


Fig. 11. Section of core log illustrating a bioclastic limestone unit and bounding surfaces, and minor flooding surfaces within overlying bioturbated siliciclastic sandstones (Winterborne Kingston borehole; Fig. 1A). The base of the bioclastic limestone unit is represented by an erosional surface with a firmground, *Glossifungites* ichnofacies (Fig. 12B). Minor flooding surfaces in the bioturbated siliciclastic sandstones are characterized by small landward facies dislocations (e.g. facies Ss4 juxtaposed above facies Ss3). These sandstones (937–943 m) form the lower part of a thick (14.5 m), upward-shallowing, bioturbated siliciclastic sandstone succession. Key to sedimentary structures as for Fig. 8, and key to trace fossils as for Fig. 10.

thick (10–20 m), upward-shallowing facies successions bounded by major flooding surfaces, and they are common in successions through the BSF.

Bioclastic limestones and their bounding surfaces

Three observations suggest that the bioclastic limestones are genetically unrelated to the siliciclastic sandstones that form most of the BSF: (i) the limestones are composed almost exclusively of bioclastic material and contain very little siliciclastic sediment (Knox *et al.*, 1982), (ii) the deeply eroded bases (Pickering, 1995) and basal conglomerate lags of the limestones in the Ham Hill Stone (Fig. 8) imply pronounced erosion and reworking of underlying siliciclastic deposits,

and (iii) the occurrence of chamosite ooids in the bioclastic limestones documented in core implies starvation of siliciclastic sediment (Knox *et al.*, 1982; see interpretation of oolitic ironstone facies association above). It follows from this interpretation that the surfaces which bound bioclastic limestones have stratigraphic significance, and the character of these surfaces is described and interpreted below.

Bioclastic limestones overlie upward-shallowing successions of bioturbated and weakly bioturbated siliciclastic sandstones across erosion surfaces that appear planar in core (e.g. at 945.3 m in Fig. 11), but which exhibit significant (>10 m) local relief at outcrop (e.g. the Ham Hill Stone, Fig. 8). At outcrop, the erosion surfaces are lined by thick (0.5 m) lags of large clasts (up to 0.3 m

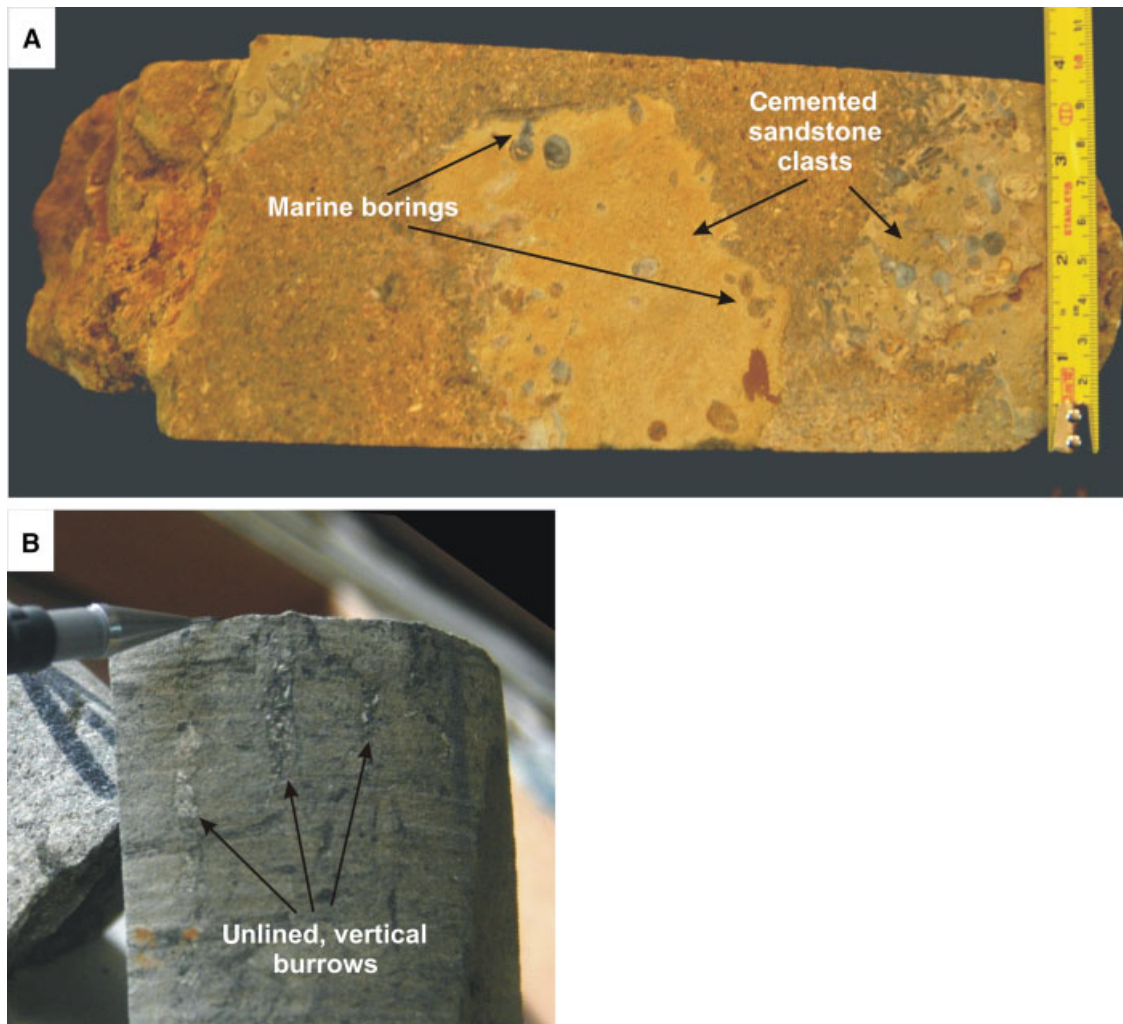


Fig. 12. Photographs illustrating characteristics of erosion surfaces at the base of bioclastic limestone units. (A) Polished surface approximately parallel to a bedding plane through a conglomerate lag lining the basal surface of the Ham Hill Stone (taken from an inactive quarry; lag corresponds to the surface at 2.6 m in Fig. 8). Large, sub-rounded clasts of cemented siliciclastic sandstones occur within a matrix of sandy, bioclastic limestone. Clasts contain marine borings around their rims. (B) Core through a firmground surface marked by unlined vertical burrows (*Glossifungites* ichnofacies) at the base of a bioclastic limestone unit (at 945.3 m in Fig. 11, Winterborne Kingston borehole; Fig. 1).

diameter) of cemented siliciclastic sandstones reworked from the underlying succession (Figs 8 and 12A). The sandstone clasts are rounded to sub-rounded, and their edges are extensively bored. The presence of these clasts implies erosional exhumation of the sandstones after cementation, followed by prolonged boring by marine organisms. In core, the basal surfaces of the limestones are marked by unlined vertical burrows (*Diplocraterion*, *Skolithos* and *Thalassinoides*) that extend up to 20 cm into the underlying siliciclastic sandstones and are infilled with bioclastic material (Figs 11 and 12B). These burrows remained open during erosional exhumation of the underlying sandstones, and thus represent a firmground, *Glossifungites* ichno-

facies developed at a hiatal surface (MacEachern *et al.*, 1992).

Interpreting the origin of the erosion surfaces at the base of the bioclastic limestones is not straightforward. The surfaces documented in core place shallow-water carbonates deposited above fair-weather wave base (bioclastic limestone facies association) directly above storm-dominated siliciclastic sediments deposited below fair-weather wave (bioturbated siliciclastic sandstone facies association). This vertical juxtaposition records abrupt shallowing of water depth, implying a basinward facies shift across a sequence boundary. Supporting evidence for this interpretation is provided at outcrop by the conglomerate lags that line the surfaces, which imply a signi-

ficant period of non-deposition and, possibly, sediment bypass during erosion. Two pieces of evidence suggest that the overlying bioclastic

limestones record subsequent transgression: (i) the absence of siliciclastic sediment and association with oolitic ironstones implies that the

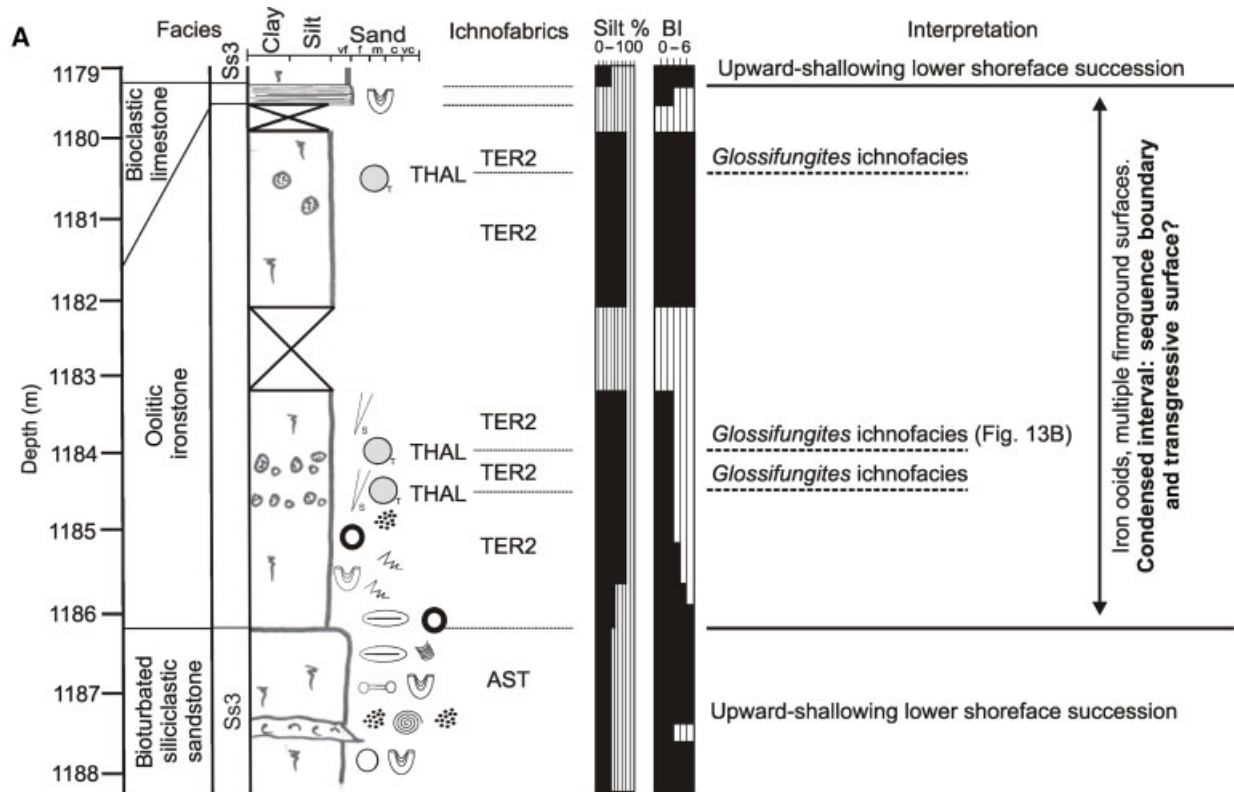


Fig. 13. (A) Section of core log illustrating facies character of an oolitic ironstone unit (Marchwood borehole; Fig. 1). The unit contains three surfaces marked by unlined *Thalassinoides* burrows (*Glossifungites* ichnofacies) infilled by bioclastic debris and iron ooids (at 1180.5–1181.0, 1184.2 and 1184.6 m in log). (B) Photograph of burrows infilled with pale bioclastic debris (at 1184.2 m in log). Key to sedimentary structures as for Fig. 8, and key to trace fossils as for Fig. 10.

bioclastic limestones formed during periods of siliciclastic sediment starvation, (ii) the limestones are overlain by, and in some instances pass gradationally upwards into, deeper-water siliciclastic deposits (distal facies of the bioturbated and weakly bioturbated siliciclastic sandstone associations; e.g. at 6.2–8.6 m in Fig. 8, 943–944 m in Fig. 11). The latter observation implies that the bioclastic limestones are overlain by flooding surfaces. Thus, the erosion surfaces at the base of the bioclastic limestones are interpreted as sequence boundaries developed during periods of relative sea-level fall, which were then reworked during subsequent transgression. There is no direct evidence that the surfaces were subaerially exposed, although such evidence (e.g. palaeosols, leaching) may have been destroyed by later transgressive erosion. The conglomerate-lined surfaces documented at outcrop are interpreted as being more proximal than the firmground surfaces observed in core, because the character of the former implies more pronounced erosion and more prolonged non-deposition, possibly within palaeovalleys (Pickering, 1995). This interpretation is consistent with regional palaeogeographic trends (e.g. Ainsworth *et al.*, 1998b; Hawkes *et al.*, 1998).

Oolitic ironstones and associated surfaces

As argued above, oolitic ironstones are interpreted as representing condensed deposition under conditions of extended physical reworking (see interpretation of oolitic ironstone facies association). In the Winterborne Kingston and the Marchwood boreholes (Fig. 1), the ironstones occur in thin (<6 m) units which coincide with major flooding surfaces that bound upward-shallowing successions of bioturbated siliciclastic sandstones (Fig. 13). In the Marchwood borehole, one oolitic ironstone unit contains several horizons of unlined *Thalassinoides* burrows infilled with bioclastic debris and hematite ooids in a matrix of green clay and sandy siltstone (Fig. 13). These burrows record the development of open burrow networks in a stiff, compacted silt substrate and later infilling by bioclastic debris and iron ooids. The burrows are interpreted as a firmground *Glossifungites* ichnofacies developed at hiatal surfaces (MacEachern *et al.*, 1992). Chamosite ooids also occur within bioclastic limestones (Knox *et al.*, 1982), suggesting a genetic link between the oolitic ironstone and bioclastic limestone facies associations.

In combination, these interpretations suggest that units of oolitic ironstone occur at major flooding surfaces as the distal equivalents to bioclastic limestones. It is possible that oolitic ironstones may record sequence boundaries reworked during later transgression, as the bioclastic limestone units are interpreted, although there is no direct evidence of lowered relative sea-level during their deposition. However, the high supply of iron needed to form the iron ooids may have resulted from the reworking of widespread lateritic palaeosols (e.g. Hallam, 1975), which would have been developed preferentially at sequence boundaries. In other basins, oolitic ironstones have been documented at sediment-starved sequence boundaries that underwent subsequent transgressive reworking (e.g. Taylor *et al.*, 2002) and at a range of other hiatal stratigraphic surfaces (e.g. Burkhalter, 1995).

Seismic-stratigraphic architecture in the Wytch Farm Field

3D seismic data over the Wytch Farm Field (Fig. 1B) allow large-scale features of the stratal architecture in the BSF to be elucidated. The Toarcian regressive–transgressive cycle consisting of the DCC, BSF and IOF is represented by approximately five wavelets (Fig. 14), which corresponds to a twofold increase in vertical resolution over regional 2D seismic data.

The 3D seismic data reveal two sets of eastward-dipping clinoform surfaces within the Toarcian regressive–transgressive cycle (clinoforms 1–5 in a lower set and clinoforms 6–7 in an upper set, Fig. 14). Clinoform surfaces are contiguous through the BSF and underlying DCC, confirming that the two units are genetically related (Fig. 14). The lower set of clinoforms (clinoforms 1–5, Fig. 14) downlap on to the underlying Junction Bed. This clinoform set is truncated at the base of the overlying IOF in the western part of the study area, where each clinoform spans the entire Bridport Sand–DCC interval (clinoforms 1–2, Fig. 14). The set exhibits a ‘downstepping’, offlapping stratal architecture within the DCC in the eastern part of the study area (clinoforms 3–5, Fig. 14). The upper set of clinoforms (clinoforms 6–7, Fig. 14) is only present in the eastern part of the study area, where it constitutes the BSF and uppermost DCC. Clinoform surfaces in the upper set downlap on to the top of the lower clinoform set and are truncated by the overlying IOF.

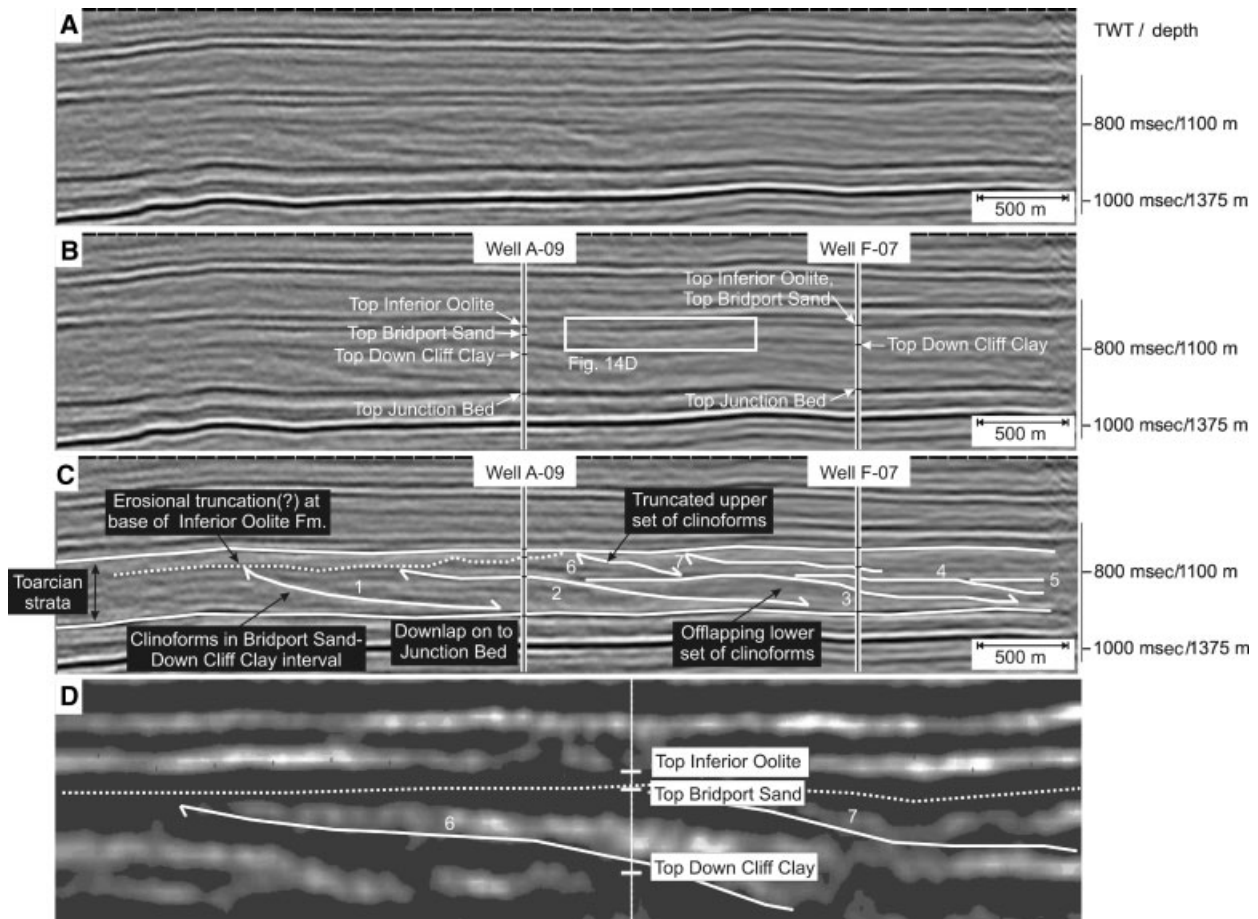


Fig. 14. Seismic-stratigraphic architecture of the Toarcian strata in the Wytch Farm Field (Fig. 1). (A) Uninterpreted west-east trending line (located in Fig. 1B) across the 'central terrace' area of the field. The same line is shown with the following annotations: (B) lithostratigraphic picks from calibrated wells, and (C) seismic-stratigraphic interpretation of clinoform surfaces through the Bridport Sand Formation and Down Cliff Clay. Clinoforms are arranged in two sets (clinoforms 1–5 in a lower set and clinoforms 6–7 in an upper set) each of which records progradation with no appreciable aggradation. The two clinoform sets are stacked in an offset, progradational pattern. (D) Detail of clinoforms 6 and 7 in the upper clinoform set (location of section is shown in panel B).

Clinoforms dip at 2–3° relative to the top of the Inferior Oolite and define a slope up to 200 m in height and 7 km in length (clinoforms 1–2, Fig. 14). In plan view, clinoforms are mapped as linear to slightly lobate features that strike roughly north–south and dip to the east (clinoforms 1–4 in the lower set, Fig. 15C) or that strike northwest–southeast and dip to the northeast (clinoforms 6–7 in the upper set, Fig. 15C). The clinoform dips are relatively steep (e.g. shoreface-shelf clinoforms typically have dips much lower than 1° over most of their length; Walker & Plint, 1992; Hampson & Storms, 2003), but there is no clear evidence of truncation surfaces in the upper slope and/or mounded deposits at the toe-of-slope to suggest the presence of slope canyons or slope collapse deposits. Clinoform surfaces have a relatively

wide spacing (*ca* 1 km) along depositional dip. Within the BSF, which is composed of bioturbated siliciclastic sandstone deposits, clinoforms are observed in wireline-log data to coincide with siltstone-dominated intervals (DcC-t facies, Table 1) above major flooding surfaces.

Clinoform distribution records overall progradation of the Bridport Sand-DCC shoreface and slope towards the east. Two discrete episodes of progradation are recorded in the Wytch Farm Field 3D seismic data set, each represented by a clinoform set (clinoforms 1–5 in a lower set and clinoforms 6–7 in an upper set, Figs 14 and 15). The two clinoform sets are stacked in an offset, progradational pattern, which implies low net accommodation during overall progradation of the Bridport Sand-DCC system. Within each

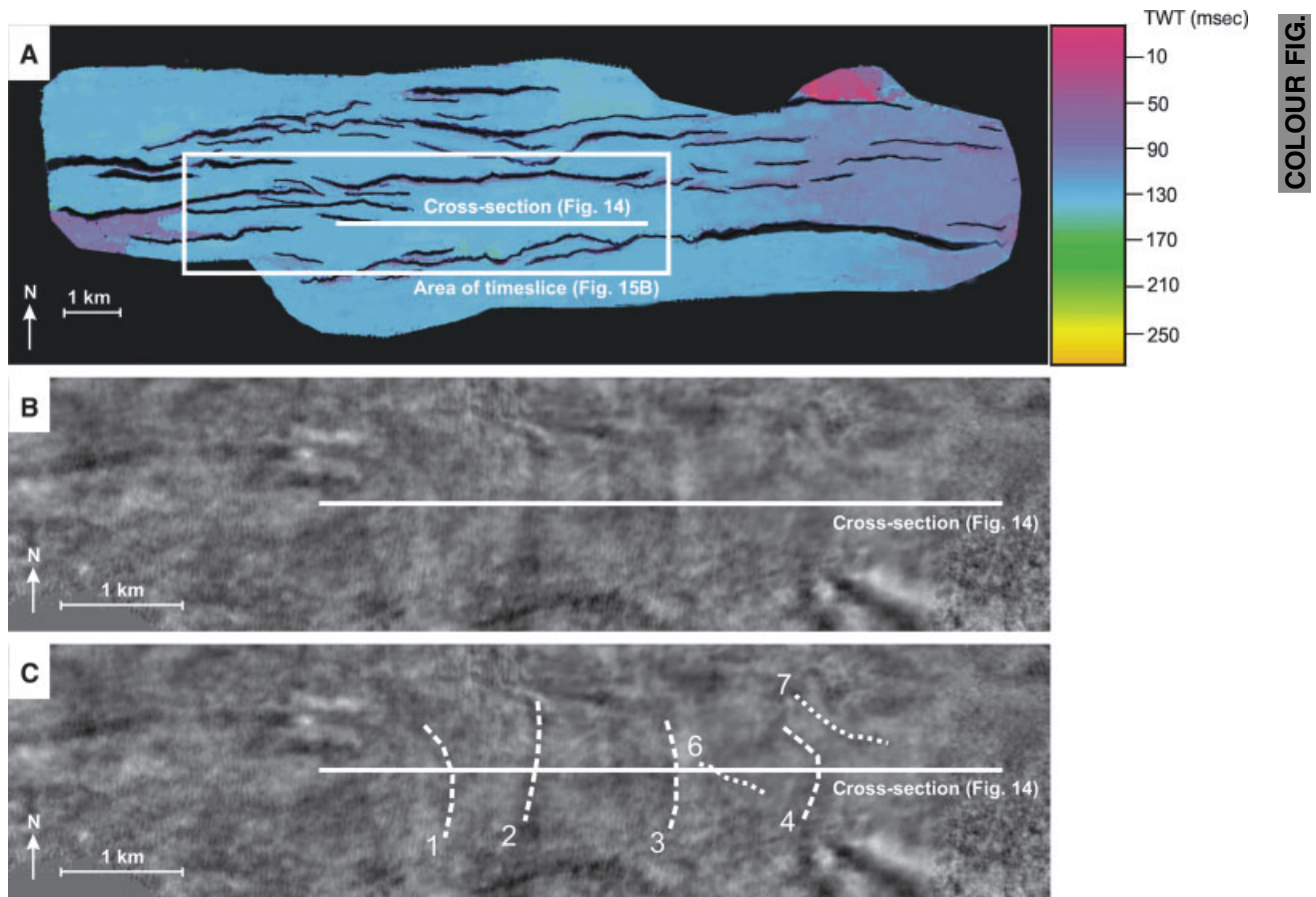


Fig. 15. (A) Isopach map of Toarcian strata (Down Cliff Clay, Bridport Sand Formation and Inferior Oolite Formation) in the Wytch Farm Field (Fig. 1), based on 3D seismic data. Note the near-constant thickness of these strata across the field, indicating that major faults were inactive during Toarcian deposition. (B) Uninterpreted and (C) interpreted timeslice through the 3D seismic volume showing the plan view distribution and trend of mapped clinoform surfaces. The timeslice is taken at 800 ms, over a window of 780–820 ms, and cuts across clinoforms 1, 2, 3, 4, 6 and 7 labelled in Fig. 14C.

clinoform set, the clinoform surfaces themselves represent major flooding surfaces that punctuated shoreface-slope progradation. The clinoform sets lack topsets, indicating that there was no appreciable aggradation as the shoreface and slope prograded, and the lower set has a 'downstepping', offlapping stratal architecture in the eastern part of the study area. Both stratal architectures are typical of progradation during conditions of falling relative sea-level (i.e. forced regression *sensu* Posamentier *et al.*, 1992) during which no accommodation is generated landward of the shoreface (e.g. Posamentier & Morris, 2000). This interpretation implies that each clinoform set represents an episode of forced regression, with a sequence boundary characterized by subaerial exposure and fluvial incision at its top (i.e. at the top of the BSF; Plint & Nummedal, 2000; Posamentier & Morris, 2000). Although there is no direct evidence for

such subaerial exposure and/or fluvial incision, this interpretation implies the bypass of anomalously large volumes of sediment to the Bridport Sand-DCC shoreface and slope during its progradation, as interpreted previously by Hesselbo & Jenkyns (1998). The truncation of each clinoform set at the base of the IOF is also consistent with widespread erosion at top-Bridport Sand level, although it may also be attributed to transgressive erosion at the base of the IOF.

Stacked clinoform sets, each 20–50 m thick, have been seismically imaged in the bioturbated-to-stratified sandstones of the Sognefjord Formation, offshore Norway (Dreyer *et al.*, 2005). Although the clinoforms are thinner than those in the Bridport Sand-DCC interval, their morphologies are similar; the Sognefjord Formation clinoforms are linear to slightly curved along strike and dip at 1–4° (locally up to 8°).

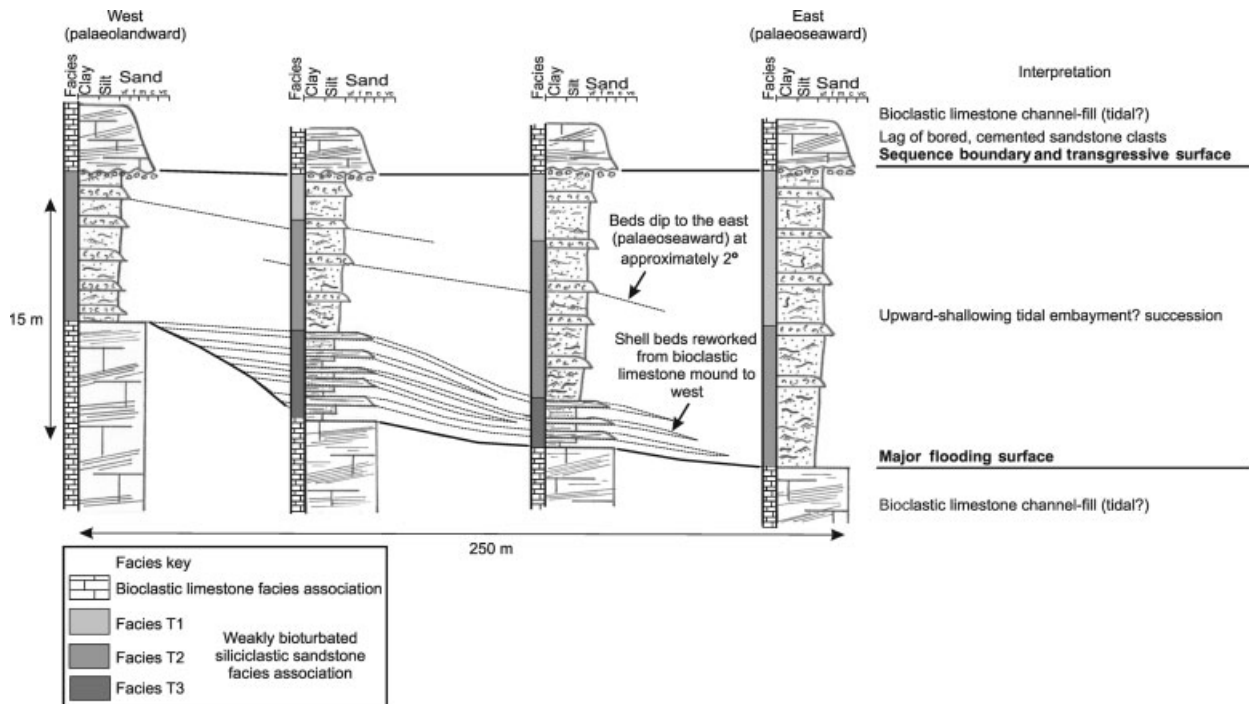


Fig. 16. Correlation panel illustrating stratigraphic architecture at Ham Hill Quarry (Fig. 1), where the Bridport Sand Formation contains an upward-shallowing succession of weakly bioturbated siliciclastic sandstones which is underlain and overlain by bioclastic limestone units. Material from the lower bioclastic limestone unit interfingers with the overlying siliciclastic succession, suggesting reworking of an original bioclastic mound. The upward-shallowing siliciclastic succession is truncated by the overlying bioclastic limestone unit. Note that carbonate-cemented beds within the siliciclastic succession have a depositional dip of *ca* 2° to the east, relative to the base of the upper limestone unit. Key to sedimentary structures as for Fig. 8.

The clinoforms occur in upward-shallowing, shelf to wave-dominated spit deposits, which are comparable with the lower shoreface and offshore transition environments interpreted for the bioturbated siliciclastic sandstones of the BSF, although the Sognefjord Formation also contains stratified upper shoreface and fore-shore deposits. The Bridport Sand-DCC clinoforms are comparable in scale and geometry to those described in the exposed Barremian and Eocene strata of Spitsbergen (1–4° dip, defining a slope >100 m in height and 3–5 km in length; Helland-Hansen, 1992; Mellere *et al.*, 2002; Steel *et al.*, 2000). In these well-documented strata, sand-prone, storm/wave-dominated deposits of broadly comparable sedimentological character to the BSF occur in relatively gently dipping (<2°) clinoform sets that record progradation coincident with aggradation of coastal-plain topsets (facies association 2 of Helland-Hansen, 1992; type 3 clinothems of Steel *et al.*, 2002). Sets of steeper clinoforms (3–4° dip) contain river-dominated deltaic and slope turbidite deposits and record forced-regressive progradation, similar in architecture

to each Bridport Sand-DCC clinoform set (facies association 1 of Helland-Hansen, 1992; type 2 clinothems of Steel *et al.*, 2002). Thus, the Bridport Sand-DCC clinoforms appear anomalous in being steep (2–3° dip) but storm/wave-dominated. Their steep geometry is interpreted as reflecting high sediment supply to the clinoform top, consistent with their forced regressive architecture. However, it is inferred that sediment was supplied to the Bridport Sand-DCC clinoforms by storm/wave processes, possibly with a strong along-shore component of transport (as in the Sognefjord Formation spit shorelines; Dreyer *et al.*, 2005), rather than by river-mouth processes. The apparent absence of slope and basin-floor fan deposits in the DCC is also consistent with the inferred lack of density currents produced by high river-mouth discharge.

Stratigraphic architecture in cliff and quarry-face exposures

Stratigraphic architecture can also be observed, albeit in a more piecemeal fashion, at outcrop.

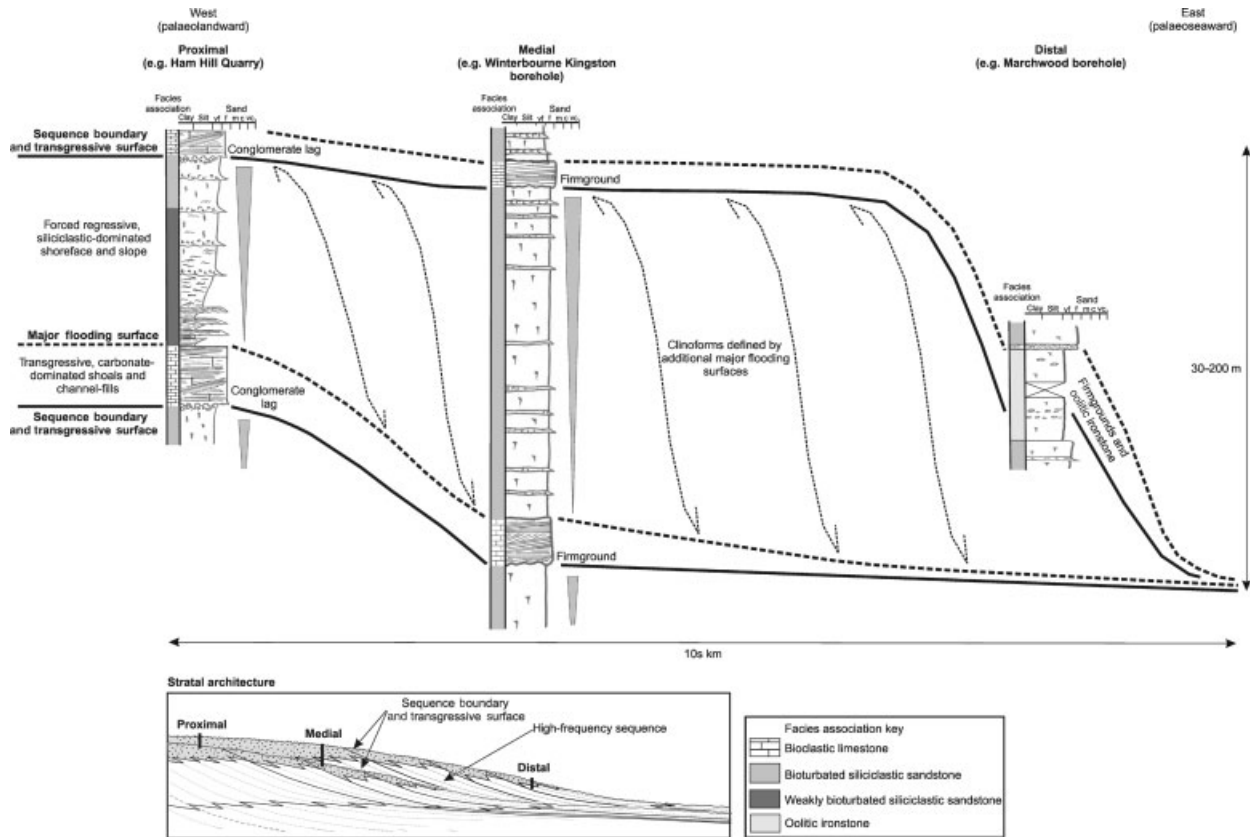


Fig. 17. Schematic correlation of representative logged sections from proximal, medial and distal locations in a single high-frequency sequence bounded by erosional unconformities and their distal correlatives in the Bridport Sand Formation. Facies successions bounded by key surfaces exhibit a consistent proximal-to-distal trend across the correlation from west to east. Representative logged sections are taken from 'type' sections at outcrop and in core, but these 'type' sections are probably taken from different high-frequency sequences. Biostratigraphic resolution and 3D seismic coverage are currently insufficient to constrain unique regional correlations of high-frequency sequences of the type portrayed schematically here. Key to sedimentary structures as for Fig. 8.

Figure 16 illustrates the stratigraphic architecture in Ham Hill Quarry (Fig. 1), where an upward-shallowing succession of weakly bioturbated siliciclastic sandstones is underlain and overlain by bioclastic limestone units. The upward-shallowing siliciclastic succession is truncated by the overlying bioclastic limestone unit across an interpreted sequence boundary which was reworked during subsequent transgression (Figs 8 and 12A). Beds within the siliciclastic succession dip to the east (palaeo-seaward) at $ca\ 2^\circ$ (Fig. 16). This architecture is similar to that described above in the Wytch Farm Field, in which progradational siliciclastic successions containing clinoforms (BSF) were truncated by a candidate sequence boundary at the base of a bioclastic limestone (IOF). Ham Hill Quarry exposes one such succession (Fig. 16), while two can be seen in the Wytch Farm 3D seismic data (Fig. 14).

Sea-cliff exposures at Bridport (Fig. 1) provide a thick (40 m), near-continuous section through the Bridport Sand and IOFs over a distance of 3 km. This exposed section trends west-east. Here the BSF comprises a single upward-shallowing succession of bioturbated siliciclastic sandstones in which laterally extensive calcite-cemented beds display no appreciable depositional dip relative to the base of the IOF (Davies, 1967, 1969; Bryant *et al.*, 1988; Hesselbo & Jenkyns, 1995). The cliff-face exposure is interpreted to be oriented along depositional strike, relative to clinoforms of the type described in the Wytch Farm Field (Figs 14 and 15). This interpretation implies southward progradation of a Bridport Sand-DCC shoreface and slope with a local west-east strike, and suggests that the regional Bridport Sand shoreline trend was broadly lobate (e.g. Fig. 11 in Ainsworth *et al.*, 1998b).

SEQUENCE STRATIGRAPHY

The facies successions, key stratigraphic surfaces and stratigraphic architectures documented above are integrated into a sequence stratigraphic model for a single high-frequency sequence in the BSF (Figs 17 and 18). Although this model honours all the available data, it is conceptual in the absence of some important data constraints and it contains several simplifying assumptions. Elements of high-frequency sequences can be readily identified in 1D vertical sections (cores, well-logs), 2D outcrop sections (cliff and quarry faces) and 3D seismic data (Wytch Farm Field). The model assumes that these data, collected from various locations in the Wessex Basin, are representative of the Bridport Sand depositional system and can thus be integrated into a single model. Toarcian strata are relatively uniform in thickness across the Wytch Farm Field (Fig. 15A), where stratal geometries are imaged with greatest clarity, and as a result the model implicitly assumes no differential tectonic subsidence within a high-frequency sequence. The impact of Toarcian rifting (e.g. as expressed in regional thickness variations, Fig. 2) on sequence architecture is discussed separately. The Wytch Farm Field 3D seismic data set also clearly shows that the BSF contains multiple high-frequency sequences (each expressed as a clinoform set, Fig. 14) which are offset laterally. In the absence of basin-wide 3D seismic data, it is not possible to deduce the total number of high-frequency sequences in the BSF in the Wessex Basin. In addition, neither ammonite nor microfossil biostratigraphic zonations (e.g. Ainsworth *et al.*, 1998a) offer sufficient resolution to attempt regional correlation of individual high-frequency sequences between widely spaced wells and outcrops. Thus the stacking patterns of high-frequency sequences, and the resulting low-frequency sequence architecture, are poorly defined, although some general inferences can be made and these are also discussed in a separate section.

High-frequency sequence stratigraphic model

Figure 17 presents a schematic correlation of key stratigraphic surfaces between representative logged sections. The correlation defines a single high-frequency sequence bounded by erosional unconformities and their distal correlates. Facies successions bounded by key sur-

faces exhibit a consistent proximal-to-distal trend across the correlation from west to east. Stratal relationships resolved in the Wytch Farm Field 3D seismic data set are used to constrain stratigraphic architecture between the logged sections. The correlation illustrates a model of high-frequency sequence development that is described below in five time steps (Fig. 18).

Early regression (falling stage systems tract)

Large volumes of siliciclastic sediment were supplied to a steeply dipping (2–3°), low-energy shoreface (BSF; 15–30 m thick) and mud-prone constructional slope (DCC; up to 200 m thick). In plan view, the shoreface was weakly lobate. Bioclastic debris is inferred as having accumulated in the upper shoreface, which is poorly preserved, perhaps in small shoals. During storm events, bioclasts were reworked and transported down-slope to form laterally extensive lags, which were further reworked and winnowed by continued storm activity on the seabed. The shoreface-slope system underwent strong progradation and minimal aggradation, resulting in the absence of coastal plain deposits and poor preservation of upper shoreface deposits (Fig. 18A). This architecture suggests forced regression during gradually falling relative sea-level and implies fluvial erosion into the top of the shoreface (Plint & Nummedal, 2000; Posamentier & Morris, 2000).

Late regression (falling stage through lowstand systems tracts)

Stratal architectures characterized by ‘down-stepping’, offlapping clinoform surfaces record the latest stage of shoreface-slope progradation (Figs 14C and 18B). These architectures imply pronounced forced regression during rapidly falling relative sea-level (Posamentier & Morris, 2000), which would have resulted in widespread emergence and deep fluvial incision into the shelf at a sequence boundary. The sequence boundary is marked by a conglomerate lag of cemented sandstone clasts in proximal locations, and a firmground surface across which there is an abrupt basinward facies shift in distal locations (Fig. 17).

Onset of transgression (late lowstand through early transgressive systems tract)

Transgressive deposits in the BSF comprise bioclastic limestone and oolitic ironstone facies associations, in marked contrast to the siliciclas-

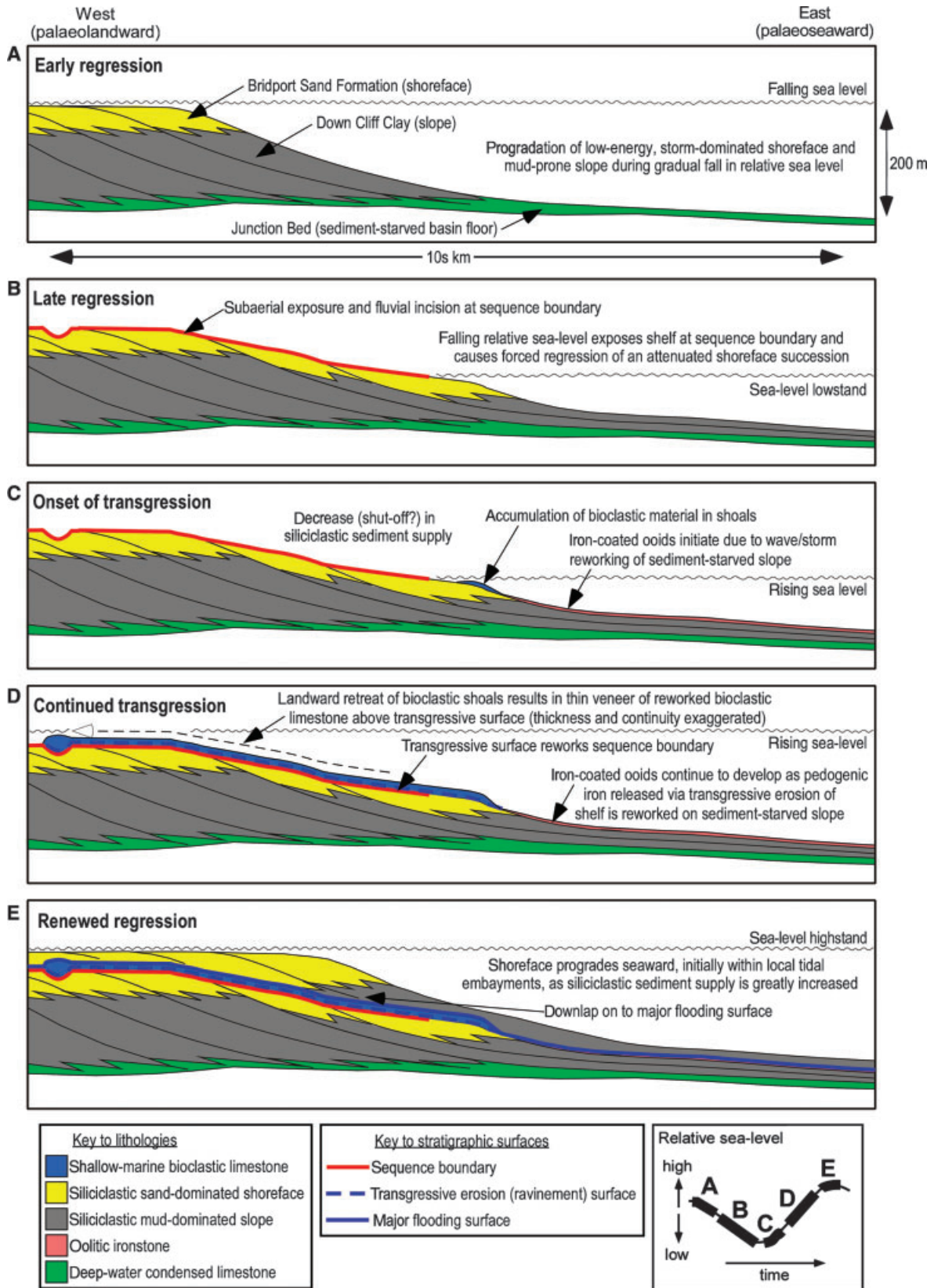


Fig. 18. Model showing development of a high-frequency sequence in the Bridport Sand Formation during a cycle of relative sea-level change: (A) early regression, (B) late regression, (C) onset of transgression, (D) continued transgression, and (E) renewed regression. See text for details.

tic deposits of the regressive deposits (Fig. 17). For this reason, transgression is interpreted as having been coincident with, and was most likely caused by, greatly decreased supply of siliciclastic sediment to the shoreface-slope system. Bioclastic material is interpreted as having accumulated in submerged shoals above the abandoned siliciclastic shoreface, and iron ooids were formed by physical reworking in more distal locations (Fig. 18C). Drowning and transgressive erosion of the wide, subaerially exposed shelf produced by earlier shoreface advance may have released pedogenic iron, thus providing a mechanism for iron enrichment in marine waters at this time.

Continued transgression (late transgressive systems tract)

During continued relative sea-level rise, bioclastic shoals were reworked landward over a transgressive ravinement surface (Fig. 18D), which eroded down to, and is thus coincident with, the sequence boundary produced during the preceding relative sea-level fall (Fig. 17). Abrasion and boring of bioclasts (e.g. Knox *et al.*, 1982) is testament to the long-lived and energetic character of transgressive reworking. Transgressive erosion also removed any thin veneer of coastal plain sediments deposited during the preceding regression. In proximal locations, bioclastic material was reworked, probably by tides (Davies, 1969), to infill palaeovalleys that were cut during the preceding relative sea-level fall (e.g. the Ham Hill Stone, Figs 8 and 16).

Onset of renewed regression (highstand systems tract)

Regressive deposits overlying the transgressive bioclastic limestones and oolitic ironstones are siliciclastic (Fig. 17), implying that renewed regression was caused by increased siliciclastic sediment supply to the basin. In proximal locations, the regressive siliciclastic deposits are weakly bioturbated sandstones (Fig. 17) that contain evidence of tidal action and fluctuating salinities in a sheltered environment, possibly a tidal embayment. The embayed character of the early regressive shoreline may have resulted from relict erosional topography which was not infilled during the preceding transgression. The second episode of regression is interpreted as having commenced in shallower water than the first (e.g. the upper clinoform set in Fig. 14C), until the shoreface advanced to the

edge of the shelf formed by the previous regression.

Stacking of high-frequency sequences and low-frequency sequence architecture

In the Wytch Farm Field, 3D seismic data show strongly progradational stacking of two high-frequency sequences (e.g. the two clinoform sets in Fig. 14C), in which the upper sequence is laterally offset from the lower one and also exhibits a subtly different progradation direction (e.g. the two clinoform sets in Fig. 15C). These interpretations of sequence stacking are corroborated at a regional scale by the occurrence of one high-frequency sequence within most vertical sections through the BSF at outcrop or in core (e.g. at the Bridport coastal outcrops and in the Wytch Farm Field). Exceptions occur in the Winterborne Trough and Wessex Shelf, which formed a fault-bounded depocentre containing a thick Toarcian section (Fig. 2). Here the BSF contains one or two bioclastic limestones (Figs 2B and 19) with interpreted sequence boundaries at their bases (e.g. Figs 8 and 11), thus dividing the BSF into two or three, vertically stacked high-frequency sequences. Overall, however, the strongly progradational stacking of high-frequency sequences implies deposition in a late highstand or falling stage sequence set (i.e. the late highstand or falling stage systems tract of a low-frequency sequence; terminology after Mitchum & Van Wagoner, 1991). The corresponding transgressive sequence set occurs within the lower part of the IOF, which represents the complete shut-off of siliciclastic sediment to the Wessex Basin, resulting in a widespread blanket of condensed limestones. This interpretation implies that a low-frequency sequence boundary occurs between the Bridport Sand and IOFs, and the contact between the two formations is indeed marked by a significant hiatus of several ammonite biozones (Fig. 3). This interpretation of the low-frequency sequence stratigraphy of the Toarcian strata which contain the BSF is essentially the same as that of Hesselbo & Jenkyns (1998). Near-identical stratigraphic architectures have been documented in the deltaic Jizera Formation, Bohemian Cretaceous Basin, Czech Republic (Ulicny, 2001), in which the absence of deltaic topset and fluvial deposits in forced-regressive clinoform sets is attributed to a combination of net low accommodation and transgressive erosion. Forced-regressive clinoform sets are also noted in Pleistocene lowstand deposits of the Rhone Delta

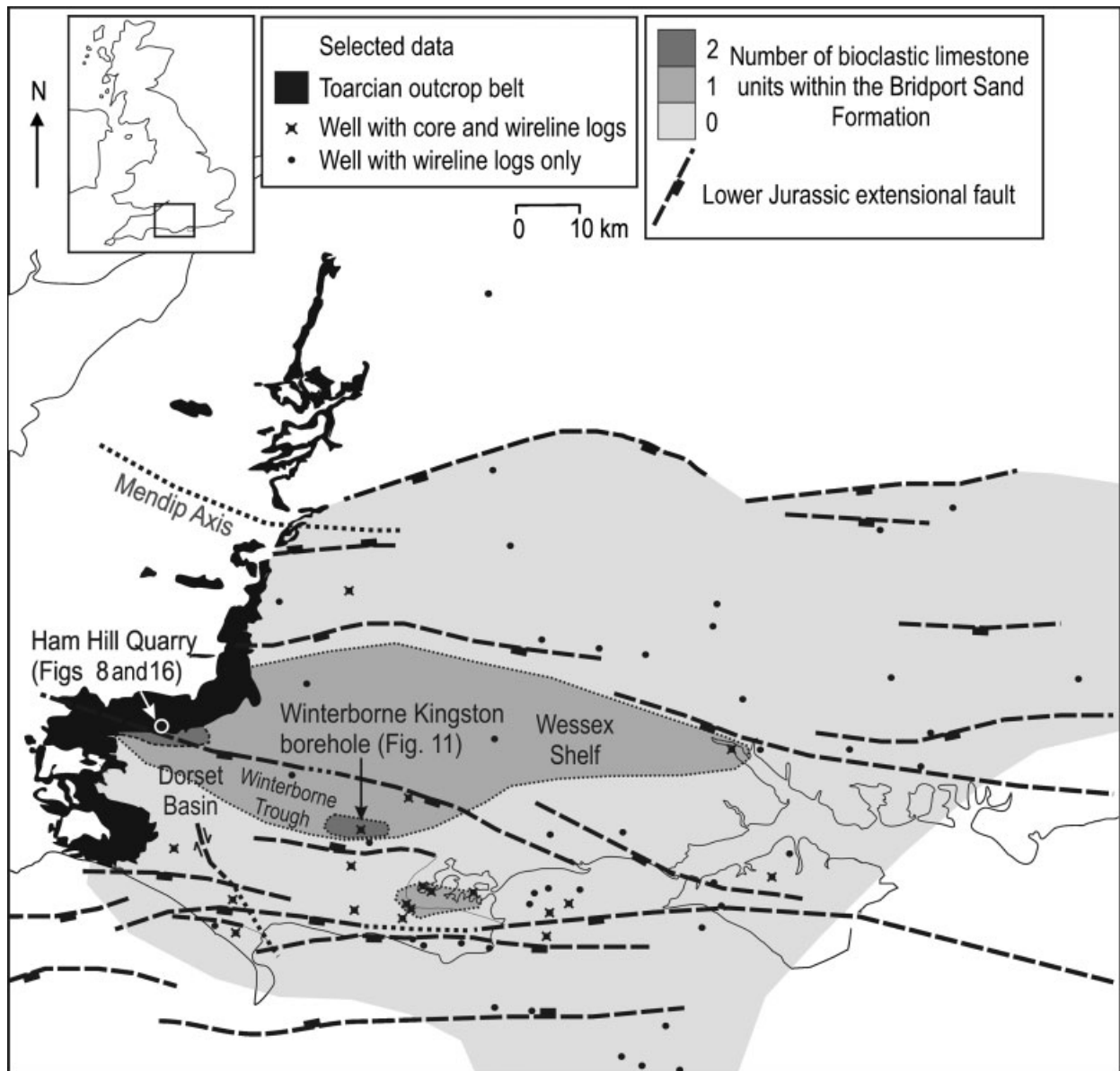


Fig. 19. Map showing the distribution of bioclastic limestone units within the Bridport Sand Formation across the Wessex Basin in relation to east–west-trending extensional faults that control the thickness of Toarcian strata (Fig. 2A). Bioclastic limestone units are documented at outcrop and in core, and are interpreted in uncored wells using wireline-log data (sonic and gamma-ray logs) as carbonate-cemented intervals over 2 m thick. Bioclastic limestones appear to occur preferentially in the fault-bounded depocentre(s) of the Wessex Shelf and Winterborne Trough.

(Posamentier *et al.*, 1992) and Central Adriatic Basin (Trincardi & Correggiari, 2000), although clinof orm sets are stacked in an aggradational to retrogradational pattern in these examples.

Structural controls on sedimentation and sequence stratigraphy

Gross regional palaeogeographies of the BSF in the Wessex Basin (Ainsworth *et al.*, 1998b;

Hawkes *et al.*, 1998) clearly show the influence of the Mendip Axis, which formed an uplifted high during the early Toarcian (Fig. 2A; Davies, 1969; Bristow *et al.*, 1999), and the adjacent Weald Basin, which formed a major fault-bounded depocentre (Fig. 2A). Within the Wessex Basin, Toarcian strata show significant thickness variations across west–east-trending extensional faults (Fig. 2) formed in response to broadly syn-depositional rifting (e.g. Dewey, 1982; Hawkes

et al., 1998). There is also clear field evidence of thickness changes in the Junction Bed and Inferior Oolite, which bound the Toarcian stratigraphic interval, across several west–east-trending extensional faults (Jenkyns & Senior, 1977, 1991). However, regional palaeogeographies show little influence of the west–east-trending structural grain within the Wessex Basin (e.g. Ainsworth *et al.*, 1998b; Hawkes *et al.*, 1998), suggesting that fault distribution was not a first-order control on sediment routing across the basin. The anomalous vertical stacking of bioclastic limestone units, interpreted as bounding high-frequency sequences, in the Winterborne Trough and Wessex Shelf (Fig. 19) is attributed to higher tectonic subsidence rates, which superposed localized aggradation on to strong regional progradation in a fault-bounded depocentre(s). This distribution suggests that bioclastic limestones did not accumulate on fault-bounded highs (e.g. the Ham Hill Stone on the footwall of a large west–east-trending fault; Fig. 19), as hypothesized by Jenkyns & Senior (1991). Instead, bioclastic limestones are interpreted as occurring above transgressively reworked, high-frequency sequence boundaries, with thick limestones (>10 m) and the tidal embayment(?) deposits that overlie them (e.g. Ham Hill Stone; Figs 8 and 16) occurring within palaeovalleys. Oolitic ironstone units in the BSF are sparse within the study data set, but appear to lack a fault-controlled distribution (e.g. Ainsworth *et al.*, 1998b). They are interpreted as occurring as the distal expression of transgressively reworked, high-frequency sequence boundaries (Fig. 18), thus their distribution reflects a stratigraphic control rather than palaeogeographic proximity to fault-induced topographic highs (e.g. Sellwood & Jenkyns, 1975; Jenkyns & Senior, 1991).

CONCLUSIONS

The study described here illustrates the value of an approach integrating ichnofabric analysis, conventional facies interpretation, 3D seismic data and sequence stratigraphy in unravelling the sedimentology and stratigraphic architecture of enigmatic, bioturbated sandstones. The main conclusions are summarized below.

1 The BSF is predominantly composed of highly bioturbated, siliciclastic silty sandstones that were deposited in a low-energy shoreface. Shoreface

deposits consist of storm-event beds that were bioturbated during fair-weather conditions, and which thus record deposition below fair-weather wave-base (i.e. in the lower shoreface and offshore transition zones). Upper shoreface and foreshore deposits are absent and/or poorly preserved.

2 The BSF shoreface was contiguous with, and passed seaward into, a large (up to 200 m), steep (2–3°), mud-dominated slope in the underlying DCC. Steep clinofold dips are attributed to high sediment supply via storm/wave processes, possibly with a strong along-shore component of transport.

3 The BSF and DCC contain multiple high-frequency sequences, each with a similar internal architecture. Sequence boundaries are defined by conglomerate lags lining deeply eroded surfaces (palaeovalleys?) in proximal locations, and by firmground surfaces with *Glossifungites* ichnofacies in distal locations. These surfaces overlie sets of ‘downstepping’, offlapping clinofolds which record forced-regressive progradation of the Bridport Sand-DCC shoreface-slope system. Each sequence boundary is interpreted as having formed during the same episode of relative sea-level fall that generated the underlying forced-regressive clinofold set. Sequence boundaries are transgressively reworked and overlain by bioclastic limestones and oolitic ironstones that record shoreline retreat during periods of siliciclastic sediment starvation. The lack of non-marine deposits in the high-frequency sequences is attributed to the absence of accommodation on the coastal plain during forced regression, combined with subsequent erosion during transgression. The latter is also invoked to account for the absence of evidence for subaerial exposure at sequence boundaries. Aspects of this high-frequency sequence model are generic and can be applied to other pervasively bioturbated sandstones.

4 High-frequency sequences are laterally stacked in a strongly progradational pattern, indicating deposition under overall conditions of high siliciclastic sediment supply and low accommodation. Aggradational stacking of high-frequency sequences occurred locally in fault-bounded depocentres with higher tectonic subsidence rates.

ACKNOWLEDGEMENTS

This work was funded by UK Natural Environment Research Council and BP via a PhD stu-

dentship for J. E. M. We thank David Richards and Gavin Ward (BP) for providing data from the Wytch Farm Field, and Bo Henk (Pacheron Group), Peter Sixsmith (Chevron) and Charlotte Robinson (Reservoir Management Ltd) for discussions of ichnofabric analysis, sequence stratigraphic models and seismic data set processing, respectively. Gavin Ward and Bo Henk first recognized the significance of clinofolds within the Bridport Sand Formation, and these ideas were developed further by Michael Hyde in an MSc project at Imperial College London. We also thank Hugh Prudden for sharing his insight into the Bridport Sand Formation outcrops, BGS staff at Keyworth for their assistance in the core store, and Nigel Ainsworth and Les Riley (BVR International Ltd) for palynological analyses. We are grateful to reviewers Stephen Hesselbo and Tom McKie and editor Peter Haughton for their insightful, rigorous and encouraging comments.

REFERENCES

- Adams, A.E., MacKenzie, W.S. and Guilford, C. (1984) *Atlas of Sedimentary Rocks Under the Microscope*. Longman Scientific & Technical, Harlow, 103 pp.
- Ainsworth, N.R., Braham, W., Gregory, J.F., Johnson, B. and King, C. (1998a) A proposed latest Triassic to earliest Cretaceous microfossil biozonation for the English Channel and its adjacent areas. In: *Development, Evolution and Petroleum Geology of the Wessex Basin* (Ed. J.R. Underhill), *Geol. Soc. London Spec. Publ.*, **133**, 87–102.
- Ainsworth, N.R., Braham, W., Gregory, J.F., Johnson, B. and King, C. (1998b) The lithostratigraphy of the latest Triassic to earliest Cretaceous of the English Channel and its adjacent areas. In: *Development, Evolution and Petroleum Geology of the Wessex Basin* (Ed. J.R. Underhill), *Geol. Soc. London Spec. Publ.*, **133**, 103–164.
- Arkell, W.J. (1933) *The Jurassic System in Great Britain*. Clarendon Press, Oxford, 681 pp.
- Bjørkum, P.A. and Walderhaug, O. (1990) Lateral extent of calcite-cemented zones in shallow marine sandstones. In: *North Sea oil and gas reservoirs – II* (Eds A.T. Buller, E. Berg and O. Hjelmeland), pp. 331–336. Graham and Trotman, London.
- Bjørkum, P.A. and Walderhaug, O. (1993) Isotopic composition of a calcite-cemented layer in the Lower Jurassic Bridport Sands, southern England: implications for formation of laterally extensive calcite-cemented layers. *J. Sed. Petrol.*, **63**, 678–682.
- Boswell, P.G.H. (1924) The petrography of the sands of the Lias-Inferior Oolite of the west of England. *Geol. Mag.*, **61**, 246–264.
- Bristow, C.R., Barton, C.M., Westhead, R.K., Freshney, E.C., Cox, B.M. and Woods, M.A. (1999) *The Wincanton District: a Concise Account of the Geology*. British Geological Survey Memoir, England and Wales, 1:50,000 Sheet **297**, 110 pp.
- Bromley, R.G. (1996) *Trace Fossils: Biology, Taphonomy and Applications*. Chapman and Hall, London, 361 pp.
- Bryant, I.D., Kantorowicz, J.D. and Love, C.F. (1988) The origin and recognition of laterally continuous carbonate-cemented horizons in the Upper Lias Sands of southern England. *Mar. Petrol. Geol.*, **5**, 109–131.
- Buchanan, J.G. (1998) The exploration history and controls on hydrocarbon prospectivity in the Wessex basins, southern England, UK. In: *Development, Evolution and Petroleum Geology of the Wessex Basin* (Ed. J.R. Underhill), *Geol. Soc. London Spec. Publ.*, **133**, 19–37.
- Buckman, S.S. (1889) On the Cotteswold, Midford and Yeovil Sands, and the division between the Lias and Oolite. *Q. J. Geol. Soc. London*, **59**, 445–458.
- Burkhalter, R.M. (1995) Ooidal ironstones and ferruginous microbialites: origin and relation to sequence stratigraphy (Aalenian and Bajocian, Swiss Jura mountains). *Sedimentology*, **42**, 57–74.
- Callomon, J.H. and Cope, J.C. (1995) The Jurassic geology of Dorset. In: *Field Geology of the British Jurassic* (Ed. P.D. Taylor), pp. 51–103. Geological Society, London.
- Chadwick, R.A. (1986) Extension tectonics in the Wessex Basin, southern England. *J. Geol. Soc. London*, **143**, 465–488.
- Chadwick, R.A., Kenolty, N. and Whittaker, A. (1983) Crustal structure beneath southern England from deep seismic reflection profiles. *J. Geol. Soc. London*, **140**, 893–891.
- Colter, V.S. and Havard, D.J. (1981) The Wytch Farm Oilfield, Dorset. In: *Petroleum Geology of the Continental Shelf of North-West Europe; Proceedings of the Second Conference* (Eds I.V. Illing and G.D. Hobson), pp. 494–503. Heydon & Son, London.
- Cox, B.M. and Page, K.N. (2002) The Middle Jurassic stratigraphy of Wessex. In: *British Middle Jurassic Stratigraphy* (Eds B.M. Cox and M.G. Sumbler), pp. 15–111. Joint Nature Conservation Committee, Peterborough.
- Davies, D.K. (1967) Origin of friable sandstone-calcareous sandstone rhythms in the Upper Lias of England. *J. Sed. Petrol.*, **37**, 1179–1188.
- Davies, D.K. (1969) Shelf sedimentation: an example from the Jurassic of Britain. *J. Sed. Petrol.*, **39**, 1344–1370.
- Day, G.A. and Edwards, J.W.F. (1983) Variscan thrusting in the basement of the English Channel and Southwest Approaches. *Proc. Ussher Soc.*, **5**, 432–436.
- Dewey, J.F. (1982) Plate tectonics and the evolution of the British Isles. *J. Geol. Soc. London*, **193**, 371–414.
- Dott, R.H. and Bourgeois, J. (1982) Hummocky stratification: significance of its variable bedding sequences. *Bull. Geol. Soc. Am.*, **93**, 663–680.
- Dreyer, T., Whitaker, M., Dexter, J., Flesche, H. and Larsen, E. (2005) From spit system to tide-dominated delta: integrated reservoir model of the upper Jurassic Sognefjord Formation on the Troll West Field. In: *Petroleum Geology: North-west Europe and Global Perspectives. Proceeding of the 6th Conference* (Eds A.G. Doré and B.A. Vining), pp. 423–448. Geological Society, London.
- Ekdale, A.A. (1985) Paleoeology of the marine endobenthos. *Palaeogeogr. Palaeoclimatol. Palaeoecol.*, **50**, 63–81.
- Gowland, S. (1996) Facies characteristics and depositional models of highly bioturbated shallow marine siliciclastic strata: an example from the Fulmar Formation (Late Jurassic), UK Central Graben. In: *Geology of the Humber Group: Central Graben and Moray Firth, UKCS* (Eds A. Hurst, H.D. Johnson, S.D. Burley, A.C. Canham and D.S. Mackertich). *Geol. Soc. London Spec. Publ.*, **114**, 185–214.

- Hallam, A.** (1975) *Jurassic Environments*. Cambridge University Press, Cambridge, 269 pp.
- Hampson, G.J.** and **Storms, J.E.A.** (2003) Geomorphological and sequence stratigraphic variability in wave-dominated, shoreface-shelf parasequences. *Sedimentology*, **50**, 667–701.
- Hawkes, P.W., Fraser, A.J.** and **Einchcomb, C.C.G.** (1998) The tectono-stratigraphic development and exploration history of the Weald and Wessex Basin, Southern England, UK. In: *Development, Evolution and Petroleum Geology of the Wessex Basin* (Ed. J.R. Underhill), *Geol. Soc. London Spec. Publ.*, **133**, 39–65.
- Helland-Hansen, W.** (1992) Geometry and facies of Tertiary clinothems, Spitsbergen. *Sedimentology*, **39**, 1013–1029.
- Hesselbo, S.P.** and **Jenkyns, H.C.** (1995) A comparison of the Hettangian to Bajocian successions of Dorset and Yorkshire. In: *Field Geology of the British Jurassic* (Ed. P.D. Taylor), pp. 105–150. Geological Society, London.
- Hesselbo, S.P.** and **Jenkyns, H.C.** (1998) British Lower Jurassic sequence stratigraphy. In: *Mesozoic and Cenozoic Sequence Stratigraphy of European Basins* (Eds P.-C. de Graciansky, J. Hardenbol, T. Jacquini and P.R. Vail), *SEPM Spec. Publ.*, **60**, 561–581.
- Hounslow, M.W.** (1987) Magnetic fabric characteristics of bioturbated wave-produced grain orientation in the Bridport-Yeovil Sands (Lower Jurassic) of Southern England. *Sedimentology*, **34**, 117–128.
- Jenkyns, H.C.** and **Senior, J.R.** (1977) A Liassic palaeofault from Dorset. *Geol. Mag.*, **114**, 47–52.
- Jenkyns, H.C.** and **Senior, J.R.** (1991) Geological evidence for intra-Jurassic faulting in the Wessex Basin and its margins. *J. Geol. Soc. London*, **148**, 245–260.
- Kantorowicz, J.D., Bryant, I.D.** and **Dawans, J. M.** (1987) Controls on the geometry and distribution of carbonate cements in Jurassic sandstones: Bridport Sands, Southern England and Viking Group, Troll field, Norway. In: *Diagenesis of Sedimentary Sequences* (Ed. J.D. Marshall). *Geol. Soc. London Spec. Publ.*, **36**, 103–118.
- Knox, R.W.O.B., Morton, A.C.** and **Lott, G.K.** (1982) Petrology of the Bridport Sands in the Winterborne Kingston borehole, Dorset. In: *The Winterborne Kingston borehole, Dorset* (Eds G.H. Rhys, G.K. Lott and M.A. Calver), *Rep. Inst. Geol. Sci.*, **81/3**, 107–121.
- Lake, L.W., Munday, T.F.** and **Harris, R.** (1984) Lineament mapping and analysis in the Wessex Basin of Southern England: a comparison between MSS and TM data. *Proc. 10th Anniv. Int. Conf. Satellite Remote Sensing*, Reading, UK, 361–375.
- MacEachern, J.A., Raychaudhuri, I.** and **Pemberton, G.S.** (1992) Stratigraphic applications of the Glossifungites ichnofacies: delineating discontinuities in the rock record. In: *Applications of Ichnology to Petroleum Exploration; a Core Workshop* (Ed. G.S. Pemberton), *SEPM Core Workshop*, **17**, 169–198.
- Martin, M.A.** and **Pollard, J.E.** (1996) The role of trace fossil (ichnofabric) analysis in the development of depositional models for the Upper Jurassic Fulmar Formation of the Kittiwake Field (Quadrant 21 UKCS). In: *Geology of the Humber Group: Central Graben and Moray Firth, UKCS* (Eds A. Hurst, H.D. Johnson, S.D. Burley, A.C. Canham and D.S. Mackertich), *Geol. Soc. London Spec. Publ.*, **114**, 163–183.
- Mellere, D., Plink-Björklund, P.** and **Steel, R.** (2002) Anatomy of shelf deltas at the edge of a prograding Eocene shelf margin, Spitsbergen. *Sedimentology*, **49**, 1181–1206.
- Miller, W.** (1995) ‘Terebellina’ (equals *Schaubcylindrichnus freyi* ichnosp. nov.) in Pleistocene outer-shelf mudrocks of northern California. *Ichnos*, **4**, 141–150.
- Mitchum, R.M.** and **Van Wagoner, J.C.** (1991) High-frequency sequences and their stacking patterns: sequence-stratigraphic evidence of high-frequency eustatic cycles. *Sed. Geol.*, **70**, 131–160.
- Morton, A.C.** (1982) Heavy minerals from the sandstones of the Winterborne Kingston borehole, Dorset. In: *The Winterborne Kingston borehole, Dorset* (Eds G.H. Rhys, G.K. Lott and M. Calver). *Rep. Inst. Geol. Sci.*, **81/3**, 143–148.
- Pemberton, G.S.** and **MacEachern, J.A.** (1997) The ichnological signature of storm deposits: the use of trace fossils in event stratigraphy. In: *Palaeontological events; stratigraphic, ecological, and evolutionary implications* (Eds B.E. Carleton and B.C. Gordon), pp. 73–109. Columbia University Press, New York.
- Pemberton, G.S., MacEachern, J.A.** and **Frey, R.W.** (1992) Trace fossils facies models: environmental and allostratigraphic significance. In: *Facies Models – Responses to Sea Level Change* (Eds R.G. Walker and N.P. James), pp. 47–72. Geological Association of Canada, St. John’s, Newfoundland.
- Pickering, K.T.** (1995) Are enigmatic erosional sandy wave-like bedforms in Jurassic Bridport Sands, Dorset, due to standing waves? *J. Geol. Soc. London*, **152**, 481–485.
- Plint, A.G.** and **Nummedal, D.** (2000) The falling stage systems tract: recognition and importance in sequence stratigraphic analysis. In: *Sedimentary Responses to Forced Egression* (Eds D. Hunt and R.L. Gawthorpe). *Geol. Soc. London Spec. Publ.*, **172**, 1–18.
- Posamentier, H.W.** and **Morris, W.R.** (2000) Aspects of the stratal architecture of forced regressive deposits. In: *Sedimentary Responses to Forced Regressions* (Eds D.G. Hunt and R.L. Gawthorpe), *Geol. Soc. London Spec. Publ.*, **172**, 19–46.
- Posamentier, H.W., Allen, H.W., James, D.P.** and **Tesson, M.** (1992) Forced regressions in a sequence stratigraphic framework: concepts, examples and sequence stratigraphic significance. *AAPG Bull.*, **76**, 1687–1709.
- Prudden, H.C.** (1967) Excavations in the Yeovil Sands at Yew Tree Close. *Proc. Dorset Natural History Archaeological Soc.*, **88**, 42–43.
- Seilacher, A.** (1967) Bathymetry of trace fossils. *Mar. Geol.*, **5**, 413–428.
- Sellwood, B.W.** and **Jenkyns, H.C.** (1975) Basin and swells and the evolution of an eperic sea (Pliensbachian-Bajocian of Great Britain). *J. Geol. Soc. London*, **131**, 373–388.
- Sellwood, B.W., Scott, J.** and **Lunn, G.** (1986) Mesozoic basin evolution in Southern England. *Proc. Geol. Assoc.*, **97**, 259–289.
- Steel, R., Mellere, D., Plink-Björklund, P., Crabaugh, J., Deibert, J.** and **Schellpeper, M.** (2000) Deltas versus rivers on a shelf edge: their relative contributions to the growth of shelf-margins and basin-floor fans (Barremian and Eocene, Spitsbergen). In: *Deep-Water Reservoirs of the World* (Eds P. Weimer, R.M. Slatt, J. Coleman, N.C. Rosen, H. Nelson, A.H. Bouma, M.J. Styzen and D.T. Lawrence), *Transactions Gulf Coast SEPM Annual Conference*, Houston, pp. 981–1009 (CD-ROM).
- Storey, J.** (1990) The regional diagenesis of the Upper Lias Formation, Southern England. Unpublished PhD Thesis, University of Reading, Reading, UK.

- Storms, J.E.A. and Hampson, G.J.** (2005) Formative mechanisms of shoreface-shelf intra-parasequence discontinuity surfaces: sea-level, sediment supply or wave-induced? *J. Sed. Res.*, **75**, 67–81.
- Taylor, A.M. and Gawthorpe, R.L.** (1993) Application of sequence stratigraphy and trace fossil analysis to reservoir description examples for the Jurassic of the North Sea. In: *Petroleum Geology of Northwest Europe; Proceedings of the 4th Conference* (Ed. J.R. Parker), pp. 317–335. Geological Society, London.
- Taylor, A.M. and Goldring, R.** (1993) Description and analysis of bioturbation and ichnofabric. *J. Geol. Soc. London*, **150**, 141–148.
- Taylor, K.G., Simo, T., Yokum, D. and Leckie, D.A.** (2002) Stratigraphic significance of ooidal ironstones from the Cretaceous Western Interior Seaway: the Castlegate Sandstone, Utah and the Peace River Formation, Alberta. *J. Sed. Res.*, **72**, 316–327.
- Trincardi, F. and Correggiari, A.** (2000) Quaternary forced regression deposits in the Adriatic Basin and the record of composite sea-level cycles. In: *Sedimentary Responses to Forced Regressions* (Eds D.G. Hunt and R.L. Gawthorpe). *Geol. Soc. London Spec. Publ.*, **172**, 245–269.
- Ulicny, D.** (2001) Depositional systems and sequence stratigraphy of coarse-grained deltas in a shallow-marine, strike-slip setting: the Bohemian Cretaceous Basin, Czech Republic. *Sedimentology*, **48**, 599–628.
- Underhill, J.R. and Stoneley, R.** (1998) Introduction to the development, evolution and petroleum geology of the Wessex Basin. In: *Development, Evolution and Petroleum Geology of the Wessex Basin* (Ed. J.R. Underhill), *Geol. Soc. London Spec. Publ.*, **133**, 1–18.
- Van Wagoner, J.C., Mitchum, R.M., Campion, K.M. and Rahmanian, V.D.** (1990) Siliciclastic sequence stratigraphy in well logs, cores, and outcrops. *AAPG Methods in Exploration*, **7**, 55 pp.
- Walker, R.G. and Plint, A.G.** (1992) Wave and storm-dominated shallow marine systems. In: *Facies Models; Response to Sea-Level Change* (Eds R.G. Walker and N.P. James), pp. 219–238. Geological Association of Canada, St. John's, Newfoundland.
- Whittaker, A.** (ed.) (1985) *Atlas of Onshore Sedimentary Basins in England and Wales; Post-Carboniferous Tectonics and Stratigraphy*. Blackie, Glasgow, 71 pp.
- Young, T.P.** (1989) Phanerozoic ironstones: an introduction and review. In: *Phanerozoic Ironstones* (Eds T.P. Young and W.E.G. Taylor), *Geol. Soc. London Spec. Publ.*, **46**, ix–xxv.

APPENDIX: PALYNOLOGICAL ANALYSES

Two samples were analysed to assess their comparative palynology: (i) siltstones from the Down Cliff Clay, taken from core, and (ii) clay-rich siltstones from weakly bioturbated sandstones (facies T3, Table 1), Bridport Sand Formation, taken from Ham Hill Quarry (Figs 8 and 16). Both samples are barren of macrofauna.

The palynomorph assemblage in the Down Cliff Clay sample is dominated by bisaccate pollen, with significant *Classopollis/Sphaeromorphs/Spheripollenites*, and significant vitrinite. Some plant tissue and/or cuticle is present. *Tasmanites*, *Crassosphaera* and acanthomorph acritarchs are common. Microforaminifera are very common. This assemblage implies a low-energy, offshore marine palaeoenvironment with partially restricted circulation. The occurrence of *Nannoceratopsis gracilis* (rare), *Scriniocassis weberi* (common) and a low variety of proximate cysts indicates an Aalenian age.

Siltstones from the weakly bioturbated sandstone facies association (facies T3, Table 1) have a low kerogen recovery, mainly comprising inertinite with subordinate sporopollenin and minor plant tissue. Predominantly miospores were recovered, with no dinocysts or microforaminifera. Rare acanthomorph acritarchs, *Tasmanites* and *Crassosphaera* are present. This sample represents a higher energy palaeoenvironment than the Down Cliff Clay sample, with winnowing and/or siliciclastic dilution of palynomorphs. The occurrence of *Callialasporites dampieri*, *Quadreaulina anellaeformis* and overall assemblage criteria indicate a Late Toarcian to Aalenian age.

Manuscript received 18 May 2004; revision accepted 10 May 2006